J|A|C|S
COMMUNICATIONS

Published on Web 01/22/2005

Lactosylated Poly(ethylene glycol)-siRNA Conjugate through Acid-Labile β-Thiopropionate Linkage to Construct pH-Sensitive Polyion Complex Micelles Achieving Enhanced Gene Silencing in Hepatoma Cells

Motoi Oishi,[†,⊥] Yukio Nagasaki,*[,†,⊥] Keiji Itaka,[‡] Nobuhiro Nishiyama,[§] and Kazunori Kataoka*[,§]

Department of Materials Science and Technology, Tokyo University of Science, 2641 Yamazaki, Noda, Chiba 278-8510, Japan, Department of Orthopaedic Surgery, Faculty of Medicine, The University of Tokyo, 7-3-1 Hongo, Bunkyo-ku, Tokyo 113-8655, Japan, and Department of Materials Science and Engineering, Graduate School of Engineering, The University of Tokyo, 7-3-1 Hongo, Bunkyo-ku, Tokyo 113-8656, Japan

Received August 20, 2004; E-mail: kataoka@bmw.t.u-tokyo.ac.jp; nagasaki@nagalabo.jp

Nucleic acid medicines such as antisense DNAs[1] and small, interfering RNAs (siRNAs)[2] have attracted much attention as a new class of therapeutic agents. In particular, siRNAs are recently recognized as the most powerful tools for sequence-specific gene silencing via naturally occurring RNA interference (RNAi) process.[3] Nevertheless, the therapeutic value of siRNAs under in vivo conditions is still controversial due to their low stability against enzymatic degradation, low permeability across cell membrane, and preferential liver and renal clearance.[4] A major key to the therapeutic success of siRNA is believed to be the development of carrier systems achieving the modulated disposition in the body through the intravenous route as well as the smooth transport of intact siRNA into the interior of the target cell. Worth noticing in this regard is a new class of nanometric-scaled carriers (nanocarriers) of oligonucleotides formulated through the self-assembly of PEG-based block ionomers (polyion complex (PIC) micelles).[5] Both combinations of PEG-*block*-polycation/oligonucleotide and PEG-*block*-oligonucleotide (or PEG-oligonucleotide conjugate)/polycation are feasible for PIC micelle formulation with a segregated PIC core surrounded by a palisade of flexible and hydrophilic PEG layers to increase biocompatibility and enzymatic tolerability. Ligands may be installed on the periphery of the PEG palisade of the PIC micelles to increase the uptake into the target cells through a receptor-mediated endocytotic pathway.[6] A unique finding, which we would like to communicate here, is the remarkably enhanced RNAi in cultured hepatoma cells through the assembly of siRNA into smart lactosylated-PIC micelles with pH-sensitive dissolution properties, thus achieving an appreciable silencing of the target gene at an extremely low siRNA concentration.

Our strategy of formulating pH-sensitive and targetable PIC micelles of siRNA is based on the novel conjugation of siRNA with lactosylated PEG through acid-labile linkage of β-thiopropionate (Lac-PEG-siRNA; Figure 1), followed by the complexation with poly(L-lysine). Note that β-thiopropionate linkage (3-sulfanylpropionyl linkage)[7] is readily cleaved at the pH corresponding to that of the intracellular endosomal compartment (pH = 5.5).[5a] Michael addition of the 5′-thiol-modified sense RNA (firefly luciferase, pGL3-control sense sequence) toward the ω-acrylate group of the α-lactosyl-ω-acryl-PEG gave a conjugate of Lac-PEG with single-stranded RNA (Lac-PEG-ssRNA), which revealed a retarded migration in gel electrophoretic assay (Figure 2, lane 3) compared to free-sense RNA (Figure 2, lane 1) in line with

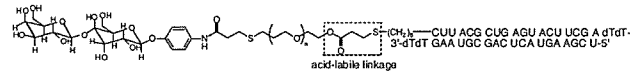

Figure 1. Chemical structure of the Lac-PEG-siRNA conjugate.

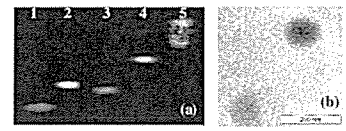

Figure 2. (a) Polyacrylamide gel retardation assay: lane 1, sense RNA; lane 2, siRNA; lane 3, Lac-PEG-ssRNA; lane 4, Lac-PEG-siRNA; and lane 5, PIC micelle. (b) Transmission electron micrograph of the disulfide cross-linked PIC micelle.

PEGylation. Then, the Lac-PEG-ssRNA was annealed with antisense RNA to undergo hybridization, preparing the Lac-PEG conjugate with siRNA (Lac-PEG-siRNA). The Lac-PEG-siRNA thus prepared gave a single band in gel electrophoresis (lane 4) and had further retarded migration compared to Lac-PEG-ssRNA (lane 3) and free siRNA (lane 2). All of these results are consistent with the successful preparation of the Lac-PEG-siRNA with negligible contamination with unreacted and intermediate compounds.

The PIC micelles from the Lac-PEG-siRNA conjugate and PLL (degree of polymerization = 40) were then prepared at the charge ratio of 1 (N/P = 1), where no free Lac-PEG-siRNA conjugate and almost complete retardation were observed in a polyacrylamide gel electrophoresis (Figure 2a, lane 5), suggesting that polyion complexation between the siRNA segment and the PLL quantitatively took place. The PIC micelle with disulfide cross-linked core was also prepared by using thiolated PLL (see Supporting Information) tolerable for the transmission electron microscopy (TEM) observation. As seen in Figure 2b, the disulfide cross-linked PIC micelles have spherical shapes with an average size (n = 36) of 117 ± 26 nm, consistent with the formation of multimolecular micellization of the Lac-PEG-siRNA with PLL.

The dual luciferase reporter assay was done in HuH-7 cells (human hepatoma cells) possessing asialoglycoprotein (ASGP) receptors, which recognize compounds bearing terminal galactose moieties,[8] to evaluate the gene silencing ability of the conjugate and the PIC micelle system (Figure 3). Both the Lac-PEG-siRNA conjugate and the PIC micelle (N/P = 1) revealed RNAi activities with a dose-dependent manner even in the presence of 10% FBS, and in particular, the PIC micelles achieved far more effective RNAi activity than the Lac-PEG-siRNA conjugate alone, viz., 50% inhibitory concentration (IC_{50}) was found to be 1.3 nM and 91.4 nM for the PIC micelle and Lac-PEG-siRNA conjugate, respec-

† Tokyo University of Science.
‡ Faculty of Medicine, The University of Tokyo.
§ Graduate School of Engineering, The University of Tokyo.
⊥ Current address: Tsukuba Research Center for Interdisciplinary Materials Science (TIMS), University of Tsukuba, 1-1-1 Tennoudai, Tsukuba, Ibaragi 305-8573, Japan.

10.1021/ja044941d CCC: $30.25

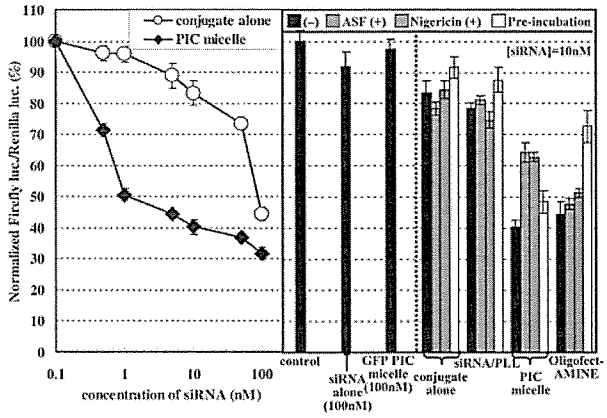

Figure 3. RNAi activities against the firefly luciferase gene generated in cultured HuH-7 cells. Normalized ratios between the firefly luciferase activity (firefly luc.) and the renilla luciferase activity (renilla luc.) are shown on the ordinate. The indicated concentrations of siRNA were the final concentrations in the total transfection volume (250 μL). The plotted data are averages of triplicate experiments ± SD. $P^* < 0.05$ (vs Lac-PEG-siRNA conjugate).

tively. This almost 100 times increase in RNAi activity by PIC micelle is remarkable.

On the other hand, no RNAi activity was observed for free siRNA even at 100 nM of siRNA concentration. The lack of RNAi activity for free siRNA may be ascribed to the low tolerability against enzymatic attack[5a] and/or the restricted uptake into the cellular interior due to the elcetrostatic repulsion with the negatively charged plasma membranes. Note that the PIC micelle including a GFP sequence induced no RNAi, strongly suggesting that an inhibition of firefly luciferase expression observed here indeed occurred through the sequence-specific RNAi effect. In addition, siRNA/PLL (polyplex) showed significantly lower RNAi activity compared to the PIC micelle probably owing to the aggregation at charge-neutralized conditions (N/P = 1) and nonspecific interaction with serum proteins. Although the RNAi activity for the PIC micelle at 10 nM of conjugate concentrations was the same level compared to the commercially available oligofectAMINE (cationic liposome), the RNAi activity for the oligofectAMINE after preincubation with 50% serum for 30 min was significantly reduced (56 → 27% inhibition, $P < 0.05$) due to the nonspecifically interacting nature of the cationic carriers with negatively charged serum proteins. In sharp contrast, the PIC micelle still retained the RNAi activity even after preincubation for 30 min with 50% serum due to the segregation of the siRNA into the PEG environment.[9] To confirm the cellular uptake pathway, asialofetuin (ASF) as the inhibitor for the ASGP receptor-mediated endocytosis[10] was added to the culture medium (4 mg/mL). As a consequence, RNAi activities were reduced significantly for the PIC micelles (60 → 36% inhibition, $P < 0.05$), whereas there was negligible effect of ASF on RNAi activities for Lac-PEG-siRNA conjugate, siRNA/PLL, and oligifectAMINE in HuH-7 cells (Figure 3). Note that no effect of ASF was observed for ASGP receptor-negative NIH 3T3 cells (mouse fibroblast) even for the PIC micelles (see Supporting Information). Obviously, these results indicate that the lactose moieties clustering on the surface of PIC micelle appreciably facilitates ASGP receptor-mediated endocytosis to direct a remarkable RNAi efficacy. Then, nigericin as the inhibitor for the endosomal acidification[11] was added to the culture medium (5 μM) to confirm that the acid-labile linkage in the conjugate contributes RNAi activity. Consequently, the RNAi activity was significantly reduced for the PIC micelle (60 → 37% inhibition, $P < 0.05$), whereas no effect was observed for the Lac-PEG-siRNA conjugate, siRNA/PLL, and the oligofectAMINE. This result suggests that after the endocytotic internalization the cleavage of the acid-labile linkage of the micelles occurred in the manner synchronized with the pH decrease in the endosomal compartment, releasing hundreds of free PEG strands to increase the colloidal osmotic pressure. This may induce the swelling and disruption of the endosome,[12] facilitating the transport of free siRNA into the cytoplasm. Several important factors are likely to be synergistically involved in the pronounced RNAi activity of the PIC micelles, such as the improvement of the stability against enzymatic degradation, minimal interaction with serum proteins, enhancement of the cellular uptake through the ASGP receptor-mediated endocytosis, and the effective transport of free siRNA from endosome into cytoplasm. It should be noted that the PIC micelles entrapping the Lac-PEG-siRNA conjugate reported here showed about 5800 times higher gene-silencing effect compared to that entrapping the Lac-PEG-antisense DNA conjugate targeting the same gene sequence (IC_{50} = 7.6 μM).[13]

In conclusion, the pH-responsive and targetable PIC micelle composed of PLL and Lac-PEG-siRNA conjugate bearing an acid-labile linkage exhibited significant gene silencing for firefly luciferase expression in HuH-7 cells. Therefore, this approach of PIC micellization of PEG-siRNA conjugate with an appropriate polycation has promise as a targetable siRNA delivery system used in a practical context. Further study on gene silencing against endogenous genes as well as in vivo performance is now in progress in our laboratories.

Acknowledgment. This work was supported by the Core Research for Evolutional Science and Technology (CREST) from the Japan Science and Technology Agency [JST]. We appreciate Mr. Teisaku Nakamura for taking the TEM image.

Supporting Information Available: Experimental details, materials, and the dual luciferase reporter assay. This material is available free of charge via the Internet at http://pubs.acs.org.

References

(1) (a) Crooke, S. T. *Biotechnol. Genet. Eng. Rev.* **1998**, *15*, 121. (b) Cook, P. D. *Handb. Exp. Pharmacol.* **1998**, *131*, 51.
(2) Elbashir, S. M.; Harborth, J.; Lendeckel, W.; Yalcin, A.; Weber, K.; Tuschl, T. *Nature* **2001**, *411*, 494.
(3) Taira, H. K. *Nucleic Acid Res.* **2003**, *31*, 700. (c) Miyagishi, M.; Taira, K. *Nat. Biotechnol.* **2002**, *20*, 497.
(4) Braasch, D.; Paroo, Z.; Constantiescu, A.; Ren, G.; Öz, O. K.; Mason, R. P.; Corey, D. R. *Bioorg. Med. Chem. Lett.* **2004**, *14*, 1139.
(5) For selected examples, see: (a) Oishi, M.; Sasaki, S.; Nagasaki, Y.; Kataoka, K. *Biomacromolecules* **2003**, *4*, 1426. (b) Jeong, J. H.; Kim, S. W.; Park, T. G. *Bioconjugate Chem.* **2003**, *14*, 473. (c) Vinogradov, S. V.; Bronich, T. K.; Kabanov, A. V. *Bioconjugate Chem.* **1998**, *9*, 805. (d) Kataoka, K.; Togawa, H.; Harada, A.; Yasugi, K.; Matsumoto, T.; Katayose, S. *Macromolecules* **1996**, *29*, 8556. (e) Harada, A.; Kataoka, K. *Macromolecules* **1995**, *28*, 5294.
(6) Wakebayashi, D.; Nishiyama, N.; Yamasaki, Y.; Itaka, K.; Kanayama, N.; Harada, A.; Nagasaki, Y.; Kataoka, K. *J. Controlled Release* **2004**, *95*, 653.
(7) Schoenmakers, R. G.; van de Wetering, P.; Elbert, D. L.; Hubbell, J. A. *J. Controlled Release* **2004**, *95*, 291.
(8) Wu, C. H.; Wu, G. Y. *Adv. Drug Delivery Rev.* **1998**, *29*, 243.
(9) Itaka, K.; Kanayama, N.; Nishiyama, N.; Jang, W.-D.; Yamasaki, Y.; Nakamura, K.; Kawaguchi, H.; Kataoka, K. *J. Am. Chem. Soc.* **2004**, *126*, 13612.
(10) Zanta, M. A.; Boussif, O.; Adib, A.; Behr, J. P. *Bioconjugate Chem.* **1997**, *8*, 839.
(11) Uherek, C.; Fominaya, J.; Wels, W. *J. Biol. Chem.* **1998**, *273*, 8835.
(12) Goh, S. L.; Murthy, N.; Xu, M.; Fréchet, J. M. J. *Bioconjugate Chem.* **2004**, *15*, 467.
(13) Oishi, M.; Nagatsugi, F.; Sasaki, S.; Nagasaki, Y.; Kataoka, K. *ChemBioChem.* In press.

JA044941D

Drug Delivery

Supramolecular Nanocarrier of Anionic Dendrimer Porphyrins with Cationic Block Copolymers Modified with Polyethylene Glycol to Enhance Intracellular Photodynamic Efficacy**

*Woo-Dong Jang, Nobuhiro Nishiyama, Guo-Dong Zhang, Atsushi Harada, Dong-Lin Jiang, Satoko Kawauchi, Yuji Morimoto, Makoto Kikuchi, Hiroyuki Koyama, Takuzo Aida, and Kazunori Kataoka**

A great number of challenges have been overcome to create efficient photosensitizers (PSs) for photodynamic therapy (PDT) which have a high photocytotoxicity and selectivity for

[*] Dr. W.-D. Jang, Dr. N. Nishiyama, Dr. G.-D. Zhang, Dr. A. Harada, Prof. Dr. K. Kataoka
Department of Materials Science and Engineering
Graduate School of Engineering, The University of Tokyo
7-3-1 Hongo, Bunkyo-ku, Tokyo 113-8656 (Japan)
Fax: (+81) 3-5841-7139
E-mail: kataoka@bmw.t.u-tokyo.ac.jp

Dr. D.-L. Jiang, Prof. Dr. T. Aida
Department of Chemistry and Biotechnology
Graduate School of Engineering, The University of Tokyo
7-3-1 Hongo, Bunkyo-ku, Tokyo 113-8656 (Japan)

Dr. W.-D. Jang, Dr. G.-D. Zhang, Dr. A. Harada, Prof. Dr. K. Kataoka
CREST
Japan Science and Technology Corporation (Japan)

Dr. N. Nishiyama, Dr. H. Koyama
Department of Clinical Vascular Regeneration
Graduate School of Medicine, The University of Tokyo
7-3-1 Hongo, Bunkyo-ku, Tokyo 113-8655 (Japan)

Dr. S. Kawauchi, Dr. Y. Morimoto, Prof. Dr. M. Kikuchi
Department of Medical Engineering
National Defense Medical College
3-2 Namiki, Tokorozawa, Saitama, 359-8513 (Japan)

[**] This work was supported by Core Research for Evolutional Science and Technology (CREST), JST.

 DOI: 10.1002/anie.200461603

the diseased tissue.[1] To obtain high quantum yields and effective energy absorption, PSs generally need to have large π-conjugation domains such as a porphyrin structure. Therefore, most conventional PSs easily form aggregates, which produce a self-quenching effect of the excited state, in aqueous medium as a result of their π–π interactions and hydrophobic characteristics. These issues can be overcome, as we reported previously, by segregating PSs into the focal core of dendrimers (dendrimer porphyrins (DPs), Figure 1b).[2] DPs are attractive for biomedical purposes because of their predictable structures, that is, their monodisperse molecular weight and tunable three-dimensional structures, and their flexibility for a high density of tailored functional groups on the periphery.[3] Indeed, third-generation DPs with 32 cationic or anionic peripheral groups exhibit a high solubility in aqueous medium and have a high quantum yield for the generation of singlet oxygen, which leads to an appreciable photocytotoxicity.[2] These advantageous features of DPs are facilitated to an even greater extent by their inclusion into stealth nanocarriers, thus improving their longevity in blood circulation and results in their gradual accumulation in solid tumors through the enhanced permeation and retention (EPR) effect.[4] Furthermore, as demonstrated here, the inclusion of DPs into a novel type of nanocarrier, that is, polymeric micelles, has led to an unprecedented increase in the photocytotoxicity without compromising either the photophysical properties of DPs in regard to their efficient photochemical reactions or the physicochemical properties of the carriers necessary for tumor-selective delivery.

A novel polymeric micelle system[5] for PDT is based on an electrostatic assembly of an anionic DP,[6] which consists of zinc porphyrin at the focal core with a third generation of poly(benzyl ether) dendritic frameworks having 32 negative charges on the periphery, and poly(ethylene glycol)–poly(L-lysine) block copolymer (PEG-*b*-PLL) in aqueous media (polyion complex (PIC) micelles; Figure 1b).[7] The DP-incorporated micelles (DP/m), prepared with a stoichiometric ratio of negatively charged DP and positively charged PEG-*b*-PLL, were approximately 64 nm in diameter with an extremely narrow size distribution in physiological saline solution (Figure 2a). Our previous study using static light scattering (SLS) measurements demonstrated that an individual DP/m contains an average of 38 DP molecules and the micelles have a remarkable stability against salt concentrations,[7] which indicates the clear stabilization effect by the 32 negative charges of DP in the micellar structure. The dependency of the formation of DP/m on the pH value was investigated by dynamic and static light scattering (DLS and SLS) measurements. Figure 2b shows the pH-dependent changes in the translational diffusion coefficient (D_T) and normalized $(Kc/\Delta R(0))^{-1}$ (normalized to the micelle at pH 7.4) of DP/m, where D_T is related to the hydrodynamic size based on the Stokes–Einstein equation, and the normalized $(Kc/\Delta R(0))^{-1}$ value is related to the changes in the average apparent molecular weight of the micelles. Both the hydrodynamic size and normalized $(Kc/\Delta R(0))^{-1}$ value basically remained unchanged in the pH range from 6.4 to 8.5 (Figure 2b). However, the diameter of the micelles gradually

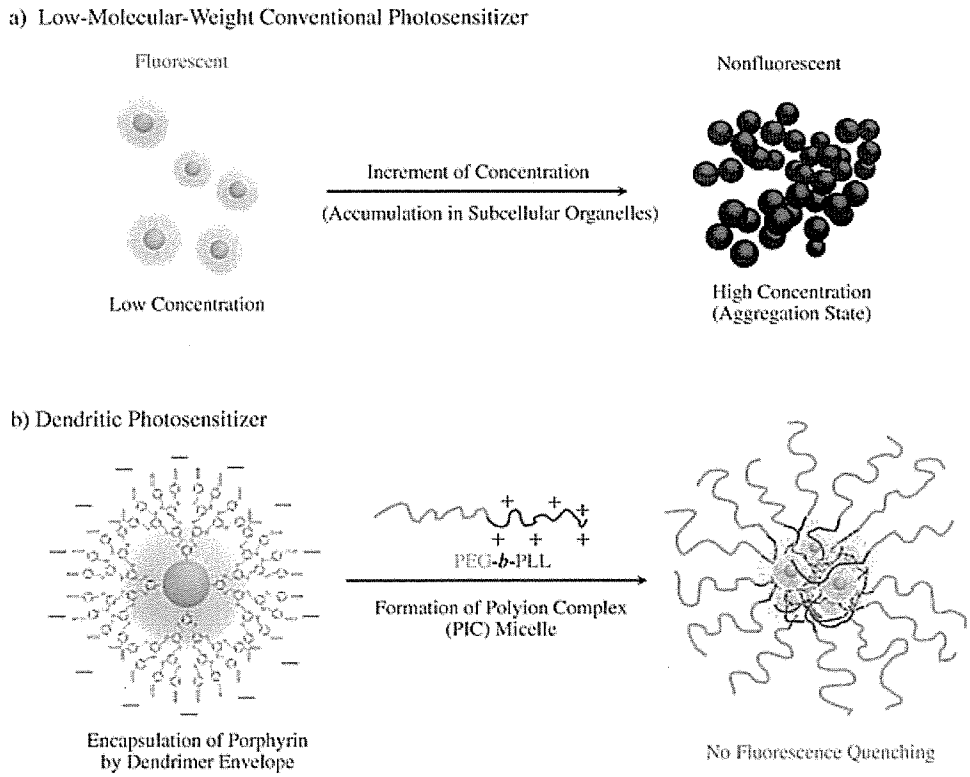

Figure 1. a) Conventional PS aggregate at a high concentration which results in quenching of PSs. b) Formation of polyion complex (PIC) micelles through electrostatic assembly of anionic dendrimer porphyrins (DPs) and PEG-*b*-PLL copolymers. The dendrimer envelope of DP can sterically prevent aggregation of the center porphyrin, thus there is no fluorescence quenching of the center porphyrin.

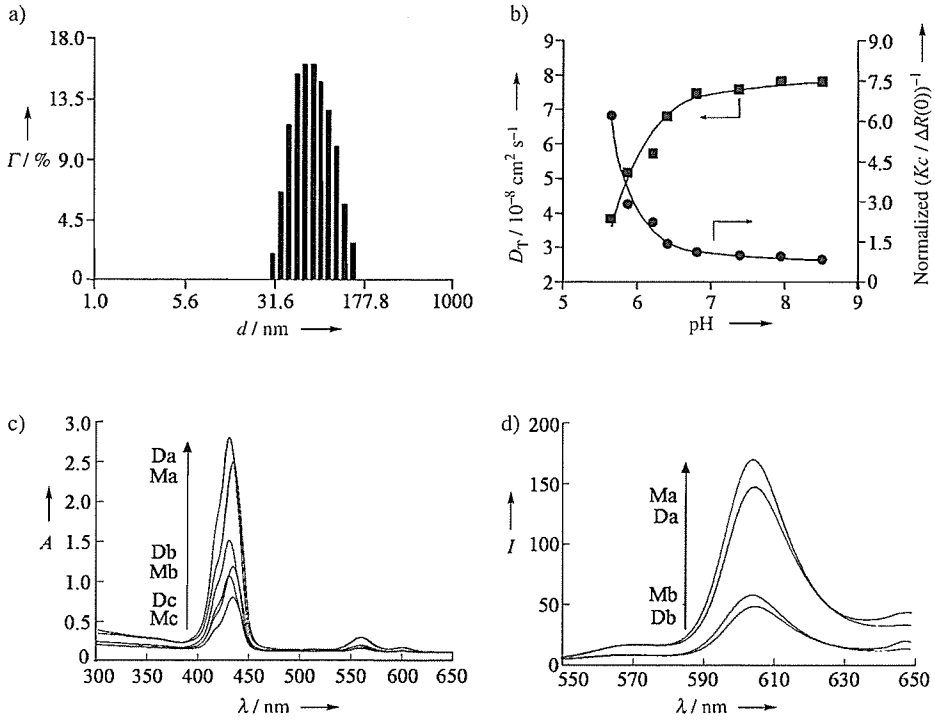

Figure 2. Physical properties of DP and DP/m. a) DLS histogram of DP/m in 150 mM NaCl at 25 °C; d = diameter. b) Dependency of the translational diffusion coefficients D_T (■) and normalized (Kc/$\Delta R(0)$)$^{-1}$ (●) on the pH value for DP/m (1 mg mL^{-1}), measured by DLS and SLS, respectively, at 25 °C. c) Electronic absorption spectra of DP alone and DP/m in PBS (pH 7.4; a = 12 μM, b = 4 μM, c = 2 μM, D: DP, M: DP/m). d) Fluorescence emission spectra of DP alone and DP/m in PBS (pH 7.4; a = 12 μM, b = 4 μM, D: DP, M: DP/m).

increased with an increased apparent molecular weight below pH 6.4 (Figure 2b), and finally precipitated at pH 5.6, which indicates the acid-responsive feature of the micelles. Protonation of DP occurred under acidic pH conditions and resulted in the diminution of the electrostatic interaction between DP and PEG-*b*-PLL. Thus, the well-defined core–shell structure may become more diffuse and a merging of the micelles may take place. This pH-responsive behavior of the micelles allows their effective accumulation in solid tumors in response to the low pH value of the tumor tissue[8] or in an endosomal compartment in the tumor cells while achieving stable circulation in the bloodstream.

The electronic absorption and emission spectra of DP and DP/m are shown in Figure 2c and d, respectively. Unlike low-molecular-weight PSs,[9] DP clearly maintained its absorption and emission intensity in spite of the formation of micelles. The incorporation of DP into the micelles resulted in a 5-nm red-shift for the Soret band of the porphyrin core and a hypochromicity of about 5% (Figure 2c). Both of these effects are likely to be caused by the formation of an electrostatic assembly of charged porphyrins and oppositely charged compounds.[10] The shrinkage of the hydrophobic dendrimer frameworks, which arises from the relaxation of the charge repulsion of the negatively charged DP surface by the formation of an electrostatic assembly, may contribute to the hypochromicity.[11] Interestingly, although the local concentration of DP within each micelle is assumed to be extremely high, DP/m emitted a more intense fluorescence at 610 nm (Figure 2d). Unlike conventional PSs, the dendritic envelope of DP is able to prevent the porphyrin core from undergoing collisional quenching, even at an appreciably high concentration that induces self-quenching of the conventional PSs (Figure 1a).[12] Thus, encapsulation of the porphyrins by the dendritic envelope in the micellar structure is most likely to prevent fluorescence quenching (Figures 1b and 2d). Also, the high microviscosity in the micellar core could restrain the internal molecular motion of DP, which might lead to the inhibition of the nonradiative decay and is related to the increased fluorescence intensity of DP/m (Figure 2d).[13] In connection with this observation, the photoinduced oxygen consumption of DP and DP/m was measured in phosphate-buffered saline (PBS) containing 10% fetal bovine serum (FBS) as a singlet oxygen acceptor (Figure 3). Very interestingly, the result revealed that the oxygen consumption level of

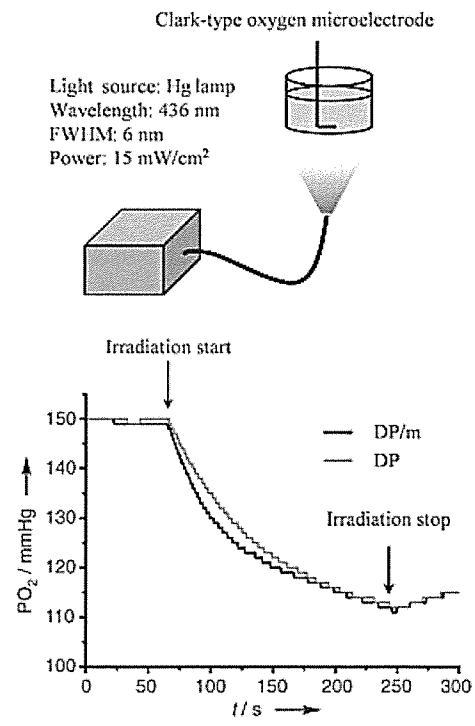

Figure 3. Experimental setup for the measurement of oxygen consumption and the results obtained. FWHM = full width of half maximum height.

DP/m was almost identical to that of the free DP in PBS, which indicates that the singlet oxygen molecules can successfully escape the micellar structure. From the standpoint of the application to PDT, the DP ensures an effective photochemical reaction of the porphyrin core regardless of the local concentrations. It is possible that the DP/m attain an elevated concentration of local singlet oxygen, which cannot be achieved by other formulations containing conventional PSs.

However, the cellular uptake of free DP and DP/m increased with the incubation time, and DP/m showed six- to eightfold higher uptake levels than free DP (Figure 4a). In

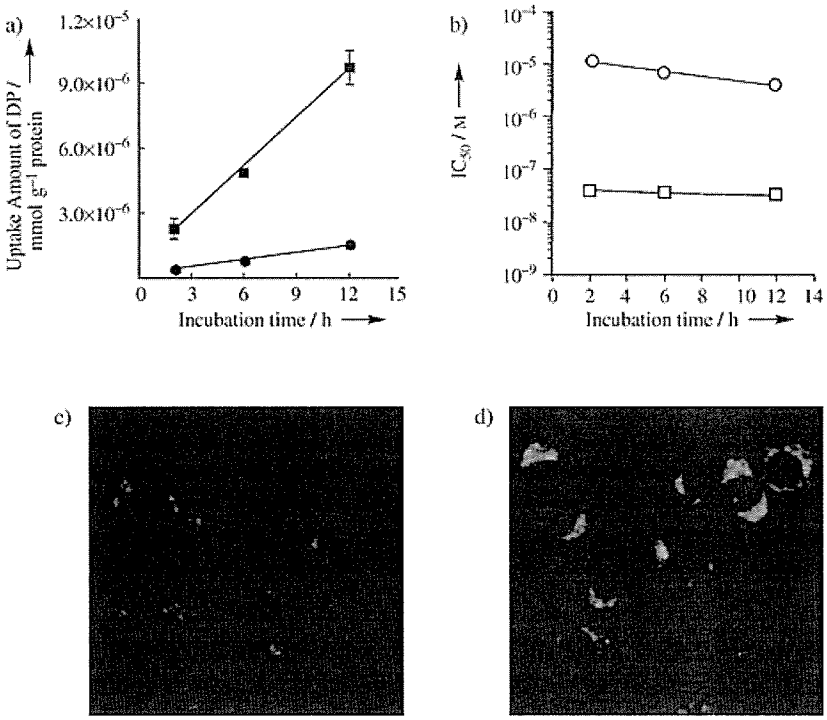

Figure 4. Results of in vitro evaluations of DP and DP/m. a) Cellular uptake level of DP (●) and DP/m (■) as a function of incubation time ($n=3$). LLC cells were incubated with dendrimers and the micelles at 12 μM of DP-equivalent concentration. b) Incubation time dependency of 50% growth inhibitory concentration (IC_{50}) of DP (○) and DP/m (□) after photoirradiation. c,d) Microscopy images of LLC cells incubated with 10 μM of DP (c) and DP/m (d) for 8 h. A Zeiss filter set (excitation: BP 395–440 nm; beam splitter: FT 460 nm; emission: LP 470 nm) was used.

view of the negatively charged surface of mammalian cells,[8] charge neutralization of DP by PEG-*b*-PLL could improve the cellular uptake of DP/m. The improved uptake of DP/m was also confirmed by microscopic observations (Figure 4c and d). No fluorescence quenching was observed for the cells incubated with DP/m, although the sensitizers are assumed to be extremely concentrated in the subcellular organelles such as the endosomes and lysosomes. This observation contrasts with the fact that the conventional mesochlorin e_6 conjugated *N*-(2-hydroxypropyl) methacrylamide (HPMA) copolymers exhibit fluorescence quenching when the cells are incubated with HPMA at an extremely high concentration.[14] The dendritic envelope of DP could prevent aggregation of the porphyrin in the subcellular loci, thus ensuring effective production of singlet oxygen for the photocytotoxicity.

Notably, the photocytotoxicity of DP/m was remarkably improved compared to that of free DP (Figure 4b). Incorporation of DP into the micelles resulted in an approximately 130–280-fold increased photocytotoxicity (Figure 4b). Such a distinctly enhanced photocytotoxicity of DP/m may not be fully explained by the six- to eightfold increase in their cellular uptake shown in Figure 4a; therefore, DP/m may have specific mechanisms to increase their photocytotoxicity. Recently, PEGylated chlorin e_6 and PEG-based polymeric micelles were reported to show an enhanced localization in several cytoplasmic organelles including the mitochondria.[15] Presumably the outer PEG layer of the DP/m and the microenvironment around DP, as mentioned above, may have a role in altering the intracellular mechanism of DP to increase the photocytotoxicity. Recently, several interesting observations concerning the intracellular mechanism have been reported. For example, Berg et al. proposed a photochemical internalization (PCI) in which the photodamage to endosomal membranes can burst the endocytic vesicles, which allows endosomal escape of macromolecules into the cytosol.[16] From this point of view, DP/m may localize in the cytoplasmic organelles susceptible to photodamage following endosomal escape of the micelles during photoirradiation. The DP/m are assumed to produce a significantly high concentration of singlet oxygen as a result of effective separation of the center porphyrin by the dendritic envelope. The mechanism for the efficient generation of singlet oxygen within the micellar structure remains to be explained. However, a dendritic structure that prevents aggregation of the center porphyrin should be essential for the enhanced photocytotoxicity of DP/m. Further investigation to address the detailed mechanisms of the enhanced photocytotoxicity of DP/m, together with dendrimer size and morphological effect, is now in progress.

In summary, the photodynamic efficacy of the DP was dramatically improved by inclusion into micelles. This process resulted in a more than two orders of magnitude increase in the photocytotoxicity compared with that of the free DP, as a result of the accumulated singlet oxygen in the intracellular compartment as well as the modulated intracellular localization related to the micellar structure. Furthermore, the DP/m system has a relevant size range (ca. 100 nm) and high stability for intravenous administration, with resultant EPR effect, and may have a high utility for in vivo PDT of cancer and macular degeneration, the study of which is now in progress.

Experimental Section

PEG-*b*-PLL was synthesized by the polymerization of the *N*-carboxy anhydride of N^{ε}-Z-L-lysine initiated by CH_3O-PEG-NH_2 (12000 g mol^{-1}) in DMF, followed by deprotection of the Z group according to a previously reported method.[17] The M_w/M_n ratio and degree of polymerization of PLL were determined to be 1.11:1 and 41 by gel-permeation chromatography and ^{1}H NMR spectroscopy,

respectively. DP was synthesized as previously described,[6] and its purity was confirmed by a single peak in the MALDI-TOF mass spectrum (8030 g mol^{-1}). The DLS and SLS measurements of DP/m were performed using a Photal dynamic laser-scattering DLS-7000 spectrometer (Otsuka Electronics Co., Ltd., Osaka, Japan). The UV/Vis and fluorescence spectra were measured on a V-550 spectrophotometer and on an FP-777 spectrofluorometer (JASCO, Tokyo, Japan), respectively.

Lewis lung carcinoma (LLC) cells were used in the cell culture studies. In the quantitative analysis of the cellular uptake of DP, the cells incubated with free DP and DP/m were lyzed in 5% SDS solution, followed by measurement of the fluorescence intensity at 609 nm (excitation at 432 nm). In the cytotoxicity assay, the cells were photoirradiated for 10 minutes with broadband visible light using a xenon lamp (150 W) equipped with a filter passing light of 400–700 nm (fluence energy: 180 kJ cm^{-2}). The viability of the cells was evaluated by the 3-(4,5-dimethylthiazol-2-yl)-2,5-diphenyltetrazolium bromide (MTT) assay.

Oxygen consumption was measured by using a Clark-type oxygen microelectrode with a tip diameter of 200 μm (PO_2-100DW, Eikou Kagaku Co., Ltd., Tokyo, Japan). The microelectrode was inserted into the PBS, which contained 3.13 μM of DP or DP/m and 10% FBS as a singlet oxygen acceptor, so that the tip was 100 mm above the bottom of the solution. An Hg lamp (436 nm, FWHM: 6 nm, 15 mW cm^{-2}) was used for light irradiation. The solution was static and exposed to the atmosphere. Before each measurement, the system was calibrated in saline solution bubbled with air, in which the oxygen partial pressure was assumed to be 150 mm Hg.

Received: August 10, 2004

Keywords: block copolymers · dendrimers · drug delivery · micelles · porphyrinoids

[1] R. K. Pandey, G. Zhang in *Porphyrin Handbook*, *Vol. 6* (Eds.: K. M. Kadish, K. M. Smith, R. Guilard), Academic Press, **2000**, pp. 157–230.
[2] N. Nishiyama, H. R. Stapert, G. D. Zhang, D. Takasu, D. L. Jiang, T. Nagano, T. Aida, K. Kataoka, *Bioconjugate Chem.* **2003**, *14*, 58–66.
[3] a) A. W. Bosman, H. M. Jassen, E. W. Meijer, *Chem. Rev.* **1999**, *99*, 1665–1688; b) S. Hecht, J. M. J. Frechet, *Angew. Chem.* **2001**, *113*, 76–94; *Angew. Chem. Int. Ed.* **2001**, *40*, 74–91; c) M. Fischer, F. Vogtle, *Angew. Chem.* **1999**, *111*, 934–955; *Angew. Chem. Int. Ed.* **1999**, *38*, 884–905; d) H. R. Ihre, L. Gagne, J. M. J. Frechet, F. C. Szoka, Jr., *Bioconjugate Chem.* **2002**, *13*, 453–461; e) J. F. Kukowska-Latallo, A. U. Bielinska, J. Johnson, R. Spindler, D. A. Tomalia, J. R. Baker, *Proc. Natl. Acad. Sci. USA* **1996**, *93*, 4897–4902.
[4] a) Y. N. Konan, R. Gurny, E. Allemann, *J. Photochem. Photobiol. B* **2002**, *66*, 89–106; b) Y. Matsumura, H. Maeda, *Cancer Res.* **1986**, *46*, 6387–6392; c) M. Yokoyama, T. Okano, Y. Sakurai, S. Fukushima, K. Okamoto, K. Kataoka, *J. Drug Targeting* **1999**, *7*, 171–186.
[5] Y. Kakizawa, K. Kataoka, *Adv. Drug Delivery Rev.* **2002**, *54*, 203–222, and references therein.
[6] a) N. Tomioka, D. Takasu, T. Takahashi, T. Aida, *Angew. Chem.* **1998**, *110*, 1611–1614; *Angew. Chem. Int. Ed.* **1998**, *37*, 1531–1534; b) T. Aida, D.-L. Jiang in *The Porphyrin Handbook*, *Vol. 3* (Eds: K. M. Kadish, K. M. Smith, R. Guilard), Academic Press, **2003**, pp. 369–384.
[7] H. R. Stapert, N. Nishiyama, D. L. Jiang, T. Aida, K. Kataoka, *Langmuir* **2000**, *16*, 8182–8188.
[8] a) E. J. Ambros, D. M. Easty, P. C. T. Jones, *Br. J. Cancer* **1958**, *12*, 439–447; b) S. E. Kornguth, T. Kalinke, H. I. Robins, J. D. Cohen, P. Turski, *Cancer Res.* **1989**, *49*, 6390–6395.
[9] S. A. Gerhardt, J. W. Lewis, D. S. Kliger, J. Z. Zhang, U. Simonis, *J. Phys. Chem. A* **2003**, *107*, 2763–2767.
[10] a) N. C. Maiti, S. Mazumdar, N. Periasamy, *J. Phys. Chem. B* **1998**, *102*, 1528–1538; b) K. M. Kadish, G. B. Maiya, C. Araullo, R. Guilard, *Inorg. Chem.* **1989**, *28*, 2725–2731.
[11] R. Sadamoto, N. Tomioka, T. Aida, *J. Am. Chem. Soc.* **1996**, *118*, 3978–3979.
[12] T. Sato, D.-L. Jiang, T. Aida, *J. Am. Chem. Soc.* **1999**, *121*, 10658–10659.
[13] S. Basu, *J. Photochem. Photobiol. A: Chem.* **1991**, *56*, 339–347.
[14] N. Nishiyama, A. Nori, A. Malugin, Y. Kasuya, P. Kopeckova, J. Kopecek, *Cancer Res.* **2003**, *63*, 7876–7882.
[15] a) M. R. Hamblin, J. L. Miller, T. Hasan, *Cancer Res.* **2001**, *61*, 7155–7162; b) R. Savic, L. Luo, A. Eisenberg, D. Maysinger, *Science* **2003**, *300*, 615–618.
[16] a) K. Berg, P. K. Selbo, L. Prasmickaite, T. E. Tjelle, K. Sandvig, J. Moan, G. Gaudernack, O. Fodstad, S. Kjolsrud, H. Anholt, G. H. Rodal, S. K. Rodal, A. Hogest, *Cancer Res.* **1999**, *59*, 1180–1183; b) L. Prasmickaite, A. Høgset, P. K. Selbo, B. Ø. Engesæter, M. Hellum, K. Berg, *Br. J. Cancer* **2002**, *86*, 652–657.
[17] A. Harada, K. Kataoka, *Macromolecules* **1995**, *28*, 5294–5299.

J|A|C|S
COMMUNICATIONS

Published on Web 09/30/2004

Supramolecular Nanocarrier of siRNA from PEG-Based Block Catiomer Carrying Diamine Side Chain with Distinctive pK_a Directed To Enhance Intracellular Gene Silencing

Keiji Itaka,[†,‡] Naoki Kanayama,[†] Nobuhiro Nishiyama,[†] Woo-Dong Jang,[†] Yuichi Yamasaki,[†] Kozo Nakamura,[‡] Hiroshi Kawaguchi,[‡] and Kazunori Kataoka*[,†]

Department of Materials Science and Engineering, Graduate School of Engineering, and Department of Orthopaedic Surgery, Faculty of Medicine, University of Tokyo, 7-3-1 Hongo, Bunkyo-ku, Tokyo 113-8656, Japan

Received May 14, 2004; E-mail: kataoka@bmw.t.u-tokyo.ac.jp

The short double-stranded RNA species, called short interference RNA (siRNA), can be used to silence the gene expression in a sequence-specific manner in a process that is known as RNA interference (RNAi).[1] It has become a useful method for the analysis of gene functions and holds the significant possibility of therapeutic application. However, to promote an efficient gene knockdown, especially in an in vivo situation, two substantial issues must be considered: tolerability under physiological conditions and enhanced cellular uptake. Thus, the development of effective siRNA delivery systems is required.

Recently, a new delivery system of plasmid DNA and oligonucleotides has been developed, based on the micellar assembly of the poly-ion complex (PIC) of these compounds with block copolymers consisting of poly(ethylene glycol) (PEG) and polycation segments, leading to the self-assembled structure with a core−shell architecture (PIC micelles).[2] Their excellent properties for in vivo DNA delivery have been confirmed so far:[3] a diameter around 100 nm with a PEG palisade which enables complexes to avoid recognition by reticuloendothelial systems, increased nuclease resistance, increased tolerance under physiological conditions, and the excellent gene expression in a serum-containing medium.[4]

We now describe the structural design of a novel block catiomer-based PIC particularly available for siRNA delivery. PEG−poly(3-[(3-aminopropyl)amino]propylaspartamide (PEG-DPT; PEG, 12 000 g/mol, polymerization degree of DPT segment, 68), carrying a diamine side chain with distinctive pK_a, was newly synthesized by a side-chain aminolysis reaction of PEG−poly(β-benzyl-L-aspartate) block copolymer (PEG-PBLA) with dipropylene triamine (DPT) (Figure 1A and Figure S1 in the Supporting Information). A model compound of a DPT unit, *tert*-butoxycarbonyl-β-*N*-3-(3-aminopropyl)aminopropylamido-α-*N*-propyl-(L)-aspartamide (Boc-Asp(DPT)-Pr), was also synthesized (see Supporting Information) to determine the pK_a values of the amino groups.

Boc-Asp(DPT)-Pr clearly gave a two-stage pH−α curve (Figure 1B), from which the pK_a values of the primary and secondary amino groups were determined to be 9.9 and 6.4, respectively. Amino groups in the PIC of polyamine with polynucleotides including siRNA generally undergo facilitated protonation due to the zipper effect or the neighboring group effect during the complexation process, hampering the proton buffering or the proton sponge capacity. The unique feature of PEG-DPT is the regulated location of primary and secondary amino groups in the side chain: the former, with higher pK_a, settles at the distal end of the side chain to participate in the ion complex formation with phosphate groups in siRNA molecule, whereas the latter, with lower pK_a, located closer to the polymer backbone, is expected to leave a substantial

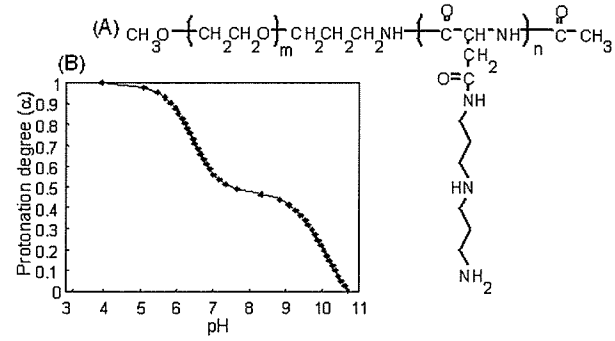

Figure 1. (A) Chemical structure of PEG-DPT. (B) Change in protonation degree (α) with pH for Boc-Asp(DPT)-Pr.

fraction of unprotonated form even in the complex, presumably due to the lower protonation power and the spatial restriction, directing to the enhanced intracellular activity of siRNA through the buffering capacity in the endosomal compartment.

The formation of the siRNA complex with the PEG-DPT was confirmed by polyacrylamide gel electrophoresis (PAGE) and the ethidium bromide (EtBr) exclusion assay (see Figure S2 in the Supporting Information). Note that intercalators such as EtBr bind the double-stranded (ds) RNA in the same fashion as dsDNA.[5] The free siRNA disappeared at the N/P ratio (= [total amines in cationic segment]/[siRNA phosphates]) >2, in line with a substantial fluorescence quenching of EtBr at N/P ≥ 2 due to the inaccessibility of EtBr to the complexed siRNA with PEG-DPT. Furthermore, the EtBr assay highlights the distinctive role of primary and secondary amino groups of the side chain in the complex. The PIC of the double-stranded oligo DNA, composed of sequences similar to the GL3 targeting siRNA, with PEG−poly(3-dimethylamino)propyl aspartamide (PEG-DMAPA; p$K_a \approx 7.9$, see Figure S3 for chemical structure), revealed a lower degree of EtBr quenching compared to the PEG-DPT/ds-oligo DNA PIC, even in the region of excess N/P ratios (see Figure S4), suggesting that the presence of unprotonated amino groups in the former may hamper the tight association. PEG−poly(L-lysine) (PEG-PLL; p$K_a \approx 9.37$, see Figure S3 for chemical structure) induced EtBr quenching as significantly as PEG-DPT upon complexation with the ds-oligo DNA, yet the quenching leveled off at the stoichiometric N/P ratio (N/P = 1.0) (Figure S4). This is in sharp contrast with the PEG-DPT/ds-oligo DNA complex, which showed leveling-off behavior of EtBr quenching at N/P $\approx$ 2.0, suggesting that secondary amines with the lower pK_a may be excluded from the ion complexation with oligonucleotides.

These distinctive features of the PEG-DPT, PEG-DMAPA, and PEG-PLL complexes indeed correlated with their gene knockdown abilities. For this evaluation, the GL3 luciferase gene was targeted

[†] Department of Materials Science and Engineering.
[‡] Department of Orthopaedic Surgery.

10.1021/ja047174r CCC: $27.50

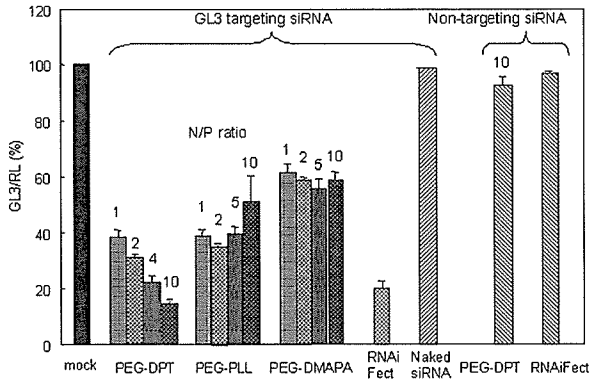

Figure 2. GL3 luciferase gene knockdown ($n = 4$; ±SD).

after transfecting two kinds of luciferase pDNAs (pGL3 and pRL; Promega) to HuH-7 cells. The expression ratio of GL3/RL was used as the knockdown marker.

Each complex system showed a sufficient knockdown of the GL3 luciferase, while neither the naked siRNA nor the nontargeting siRNA showed any knockdown (Figure 2). Thus, these results should be recognized as the veritable RNAi by the GL3-targeting siRNA delivered into the cytoplasm. Notably, the gene knockdown abilities of the siRNA/PEG-DPT complex were superior to those of the other two complexes, especially at higher N/P ratios. At N/P = 10, it showed more than an 80% knockdown, which exceeded the commercial RNAiFect. The cell viability evaluated by MTT assay was more than 75% of the mock cells, even after co-incubation with siRNA/PEG-DPT with N/P ≥ 10 (see Figure S5), suggesting the toxic effect to be eliminated. The siRNA/PEG-DMAPA complexes showed knockdown abilities to a lesser extent. Apparently, the loosely associated nature of siRNA, suggested by the EtBr exclusion assay, is unfavorable for facilitating an effective intracellular delivery of intact siRNA. PEG-PLL showed a considerable knockdown ability in the low N/P region, yet no particular enhancement with the increase in the N/P ratios. High efficacy of PEG-DPT may be characterized by the existence of additional secondary amines with a lower pK_a to promote the internalization of the siRNA molecules into the cytoplasm through buffering of the endosomal cavity, as is the case with the polyethylenimine-based polyplex that shows an enhanced tranfection efficiency at the higher N/P ratios.[6]

A serum incubation study was then performed to evaluate the complex stability under physiological conditions by incubating the complexes in 50% serum at 37 °C prior to transfection. The siRNA/PEG-DPT complexes showed comparable abilities of gene knockdown, even after co-incubation with serum for 30 min (Figure 3A). In contrast, the lipid-based RNAiFect system was significantly influenced by the serum incubation, probably due to the nonspecific association with serum proteins. Thus, these results highlighted the excellent feasibility of the PEG-DPT/siRNA complex, particularly under physiological conditions due to the segregation of siRNA into the PEG microenvironment.

The results of the endogenous gene knockdown were more fascinating. For this purpose, a cytoskeletal protein, Lamin A/C, was targeted.[1] The PEG-DPT system showed a significant gene knockdown of Lamin A/C mRNA, even after a 30-min preincubation in 50% serum, evaluated by the real-time RT-PCR analysis. Notably, in 293T cells, the expression was suppressed to the level of 20% of mock samples, which significantly exceeded the ability

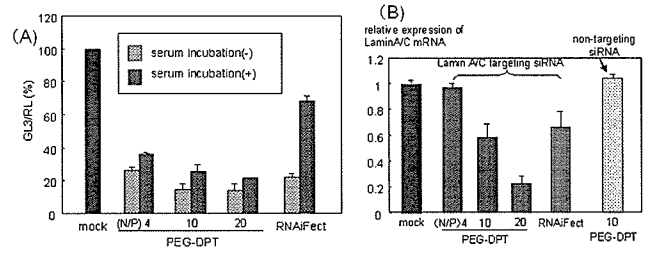

Figure 3. (A) GL3 knockdown by siRNA complexes after serum co-incubation with serum. (B) Endogenous gene (Lamin A/C) knockdown after co-incubation ($n = 4$; ±SD).

of the RNAiFect (Figure 3B). A similar trend was also observed in HuH-7 cells. However, neither the PEG-PLL nor PEG-DMAPA system showed any gene knockdown (data not shown). As Lamin A/C is assumed to abundantly express inside the cells, the threshold level of the siRNA's introduction that is necessary to show the inhibition of gene expression should be significantly higher than in the case of the luciferase cotransfection study. Thus, these results of PEG-DPT were very encouraging for the actual therapeutic knockdown of an endogenous gene by the siRNA delivering approach.

In conclusion, we reported here an effective siRNA nanocarrier system based on the self-assembly of the PEG-based block catiomer. The distinctive polymer design managed both a sufficient siRNA complexation and a buffering capacity of the endosomes. Notably, the siRNA/block catiomer complex revealed remarkable knockdown of the endogenous gene, even after the serum incubation. These results directed this newly designed system of block catiomer to have a promising feasibility for in vivo therapeutics.

Acknowledgment. This work was financially supported by the Core Research Program for Evolutional Science and Technology (CREST) from the Japan Science and Technology Corporation (JST) as well as by Special Coordination Funds for Promoting Science and Technology from the Ministry of Education, Culture, Sports, Science and Technology of Japan (MEXT).

Supporting Information Available: Detailed Materials and Methods section; ^{1}H NMR spectrum of PEG-DPT block copolymer (Figure S1); results of PAGE and EtBr exclusion assay of PEG-DPT (Figure S2); chemical structures of PEG-DMAPA and PEG-PLL (Figure S3); summary of EtBr exclusion assay of these copolymers (Figure S4); and result of MTT assay (Figure S5). This material is available free of charge via the Internet at http://pubs.acs.org.

References

(1) Elbashir, S. M.; Harborth, J.; Lendeckel, W.; Yalcin, A.; Weber, K.; Tuschl, T. *Nature* **2001**, *411*, 494−498.
(2) (a) Kataoka, K.; Togawa, H.; Harada, A.; Yasugi, K.; Matsumoto, T.; Katayose, S. *Macromolecules* **1996**, *29*, 8556−8557. (b) Katayose, S.; Kataoka, K. *Bioconjugate Chem.* **1997**, *8*, 702−707. (c) Vinogradov, S. V.; Bronich, T. K.; Kabanov, A. V. *Bioconjugate Chem.* **1998**, *9*, 805−812. (d) Choi, Y. H.; Liu, F.; Kim, J. S.; Choi, Y. K.; Park, J. S.; Kim, S. W. *J. Controlled Release* **1998**, *54*, 39−48. (e) Ogris, M.; Brunner, S.; Schuller, S.; Kircheis, R.; Wagner, E. *Gene Ther.* **1999**, *6*, 595−605. (f) Oupicky, D.; Konak, C.; Ulbrich, K.; Wolfert, M. A.; Seymour, L. W. *J. Controlled Release* **2000**, *65*, 149−171.
(3) Harada-Shiba, M.; Yamauchi, K.; Harada, A.; Takamisawa, I.; Shimokado, K.; Kataoka, K. *Gene Ther.* **2002**, *9*, 407−414.
(4) Itaka, K.; Yamauchi, K.; Harada, A.; Nakamura, K.; Kawaguchi, H.; Kataoka, K. *Biomaterials* **2003**, *24*, 4495−4506.
(5) Carlson, C.; Beal, P. A. *Biopolymers* **2003**, *70*, 86−102.
(6) Boussif, O.; Lezoualc'h, F.; Zanta, M. A.; Mergny, M. D.; Scherman, D.; Demeneix, B.; Behr, J. P. *Proc. Natl. Acad. Sci. U.S.A.* **1995**, *92*, 7297−7301.

JA047174R

J|A|C|S
ARTICLES
Published on Web 02/06/2004

Block Catiomer Polyplexes with Regulated Densities of Charge and Disulfide Cross-Linking Directed To Enhance Gene Expression

Kanjiro Miyata,[†] Yoshinori Kakizawa,[‡] Nobuhiro Nishiyama,[†,§] Atsushi Harada,[†] Yuichi Yamasaki,[†] Hiroyuki Koyama,[§] and Kazunori Kataoka*[,†,‡]

Contribution from the Department of Materials Science and Engineering, Graduate School of Engineering, The University of Tokyo, 7-3-1 Hongo, Bunkyo-ku, Tokyo 113-8656, Japan, National Institute for Materials Science, 1-1 Namiki, Tsukuba, Ibaraki 305-0044, Japan, and Department of Clinical Vascular Regeneration, Graduate School of Medicine, The University of Tokyo, 7-3-1 Hongo, Bunkyo-ku, Tokyo 113-8655, Japan

Received August 16, 2003; E-mail: kataoka@bmw.t.u-tokyo.ac.jp

Abstract: A block catiomer polyplex, showing a high stability in the extracellular medium and an efficient release of plasmid DNA (pDNA) in the intracellular compartment, was developed by controlling both the cationic charge and disulfide cross-linking densities of the backbone polycations. Poly(ethylene glycol)-poly(L-lysine) block copolymer (PEG-PLL) was thiolated using either of two thiolation reagents, *N*-succinimidyl 3-(2-pyridyldithio)propionate (SPDP) or 2-iminothiolane (Traut's reagent), to investigate the effects of both the charge and disulfide cross-linking densities on the properties of the polyplexes. The introduction of thiol groups by SPDP proceeded through the formation of amide linkages to concomitantly decrease the cationic charge density of PLL segment, whereas Traut's reagent promoted the thiolation with the introduction of cationic imino groups to keep the charge density constant. These thiolated PEG-PLLs were complexed with pDNA to form the disulfide cross-linked block catiomer polyplexes, which had the size of approximately 100 nm. Both thiolation methods were similarly effective in introducing disulfide cross-links to prevent the polyplex from the dissociation through a counter polyanion exchange in the extracellular oxidative condition. On the other hand, the efficient release of pDNA responding to the reductive condition mimicking the intracellular environment was only achieved for the polyplex thiolated with SPDP, a system compensating for the decrease in the charge density with the disulfide cross-linking. This distinctive sensitivity toward oxidative and reductive environments was nicely correlated with the remarkable difference in the transfection efficiency between these two types of thiolated polyplexes (SPDP and Traut's reagent types): the former revealed approximately 50 times higher transfection efficiency toward 293T cells than the latter. Obviously, the balance between the densities of the cationic charge and disulfide cross-linking in the thiolated polyplex played a crucial role in the delivery and controlled release of entrapped pDNA into the microenvironment of intracellular compartment to achieve the high transfection efficiency.

Introduction

Despite the current enormous interest in cationic polymer-based gene delivery systems (polyplexes), the rationale to design efficient systems has not yet been obtained. Especially, in vivo gene delivery systems through a systemic route demand a high stability during blood circulation and an efficient gene expression at the target site. Cationic block copolymers with hydrophilic segments, such as poly(ethylene glycol) (PEG), effectively induce a condensation of plasmid DNA (pDNA) upon complexation to form core−shell-type polyplexes with the hydrophilic outer layer surrounding the polyion complex (PIC) core.[1−5] This provides the increased colloidal stability to the polyplexes in a proteinaceous medium, allowing the substantial increase in their blood circulation time.[3] Nevertheless, there is still a possibility of the block catiomer polyplexes to unfavorably dissociate before entering the cytoplasm of target cells through the interaction with negatively charged biomacromolecules in the entity.[6,7] Thus, a strategy is needed to keep the polyplex structure stable in the extracytoplasmic environment, while inducing the efficient release of entrapped pDNA from the polyplexes after their movement into the cytoplasmic compartment.

[†] Graduate School of Engineering, The University of Tokyo.
[‡] National Institute for Materials Science.
[§] School of Medicine, The University of Tokyo.

(1) (a) Katayose, S.; Kataoka, K. *Advanced Biomaterials in Biomedical Engineering and Drug Delivery Systems*; Springer: Tokyo, 1996; pp 319−320. (b) Katayose, S.; Kataoka, K. *Bioconjugate Chem.* **1997**, *8*, 702−707.
(2) Wolfert, M. A.; Schacht, E. H.; Toncheva, V.; Ulbrich, K.; Nazarova, O.; Seymour, L. W. *Hum. Gene Ther.* **1996**, *7*, 2123−2133.
(3) Harada-Shiba, M.; Yamauchi, K.; Harada, A.; Takamisawa, I.; Shimokado, K.; Kataoka, K. *Gene Ther.* **2002**, *9*, 407−414.
(4) Kakizawa, Y.; Kataoka, K. *Adv. Drug Delivery Rev.* **2002**, *54*, 203−222.
(5) Kwok, K. Y.; McKenzie, D. L.; Evers, D. L.; Rice, K. G. *J. Pharm. Sci.* **1999**, *88*, 996−1003.
(6) Oupicky, D.; Howard, K. A.; Konak, C.; Dash, P. R.; Ulbrich, K.; Seymour, L. W. *Bioconjugate Chem.* **2000**, *11*, 492−501.
(7) Oupicky, D.; Carlisle, R. C.; Seymour, L. W. *Gene Ther.* **2001**, *8*, 713−724.

10.1021/ja0379666 CCC: $27.50

Scheme 1. Thiolation Schemes of PEG-PLL

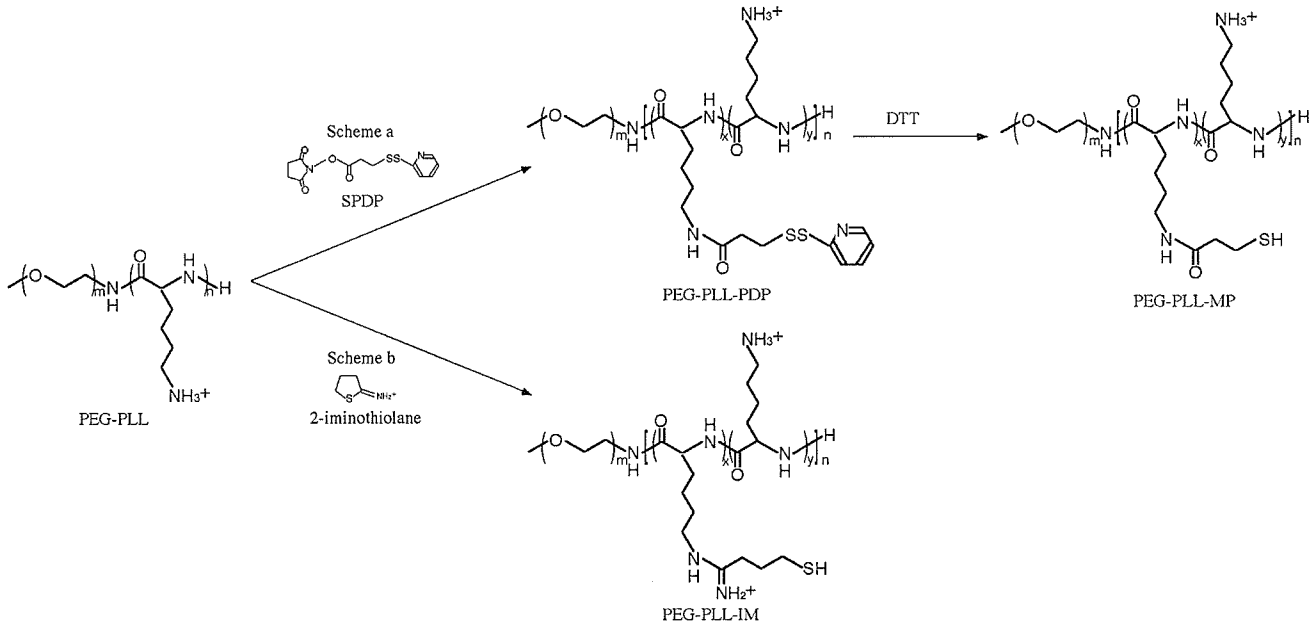

A promising approach to realize this strategy is to reversibly cross-link the PIC core of the block catiomer polyplex with disulfide bonds cleavable in intracellular reductive environments, where the glutathione concentration is ~50−1000 times higher than that in extracellular milieu.[8] Indeed, the utility of this strategy was demonstrated with the PIC of model polyanions,[9] oligo-DNA,[10] and pDNA,[7,11,12] showing that the disulfide cross-linking substantially stabilized polyplexes to achieve longevity in the blood circulation. However, the introduction of disulfide cross-links eventually led to the decreased transfection efficiency because of the overstabilization of the complex structure to hinder pDNA release in the intracellular compartment.[11] In this regard, the balance between cationic charge and disulfide cross-linking densities of the polyplex should be crucial for the disulfide cross-linked polyplexes achieving the environment-sensitive release of entrapped pDNA in the cytoplasm while maintaining its high stability in an extracellular environment. Nevertheless, previous works regarding the disulfide cross-linking of the polyplexes have not clarified this important issue, directing us to the present study devoting to design the polyplex system with regulated densities of charge and disulfide cross-linking to achieve the enhanced gene expression.

Here the charge and disulfide cross-linking densities of block catiomer polyplexes from PEG-poly(L-lysine) block copolymer (PEG-PLL) were regulated by the use of two types of thiolation reagents: *N*-succinimidyl 3-(2-pyridyldithio)propionate (SPDP)[13] and 2-iminothiolane (Traut's reagent).[14] Thiolation using SPDP proceeds by substituting amide groups for the ϵ-amino groups of the lysine residue, resulting in the decreased charge density compensated by the introduction of 3-(2-pyridyldithio)propionyl groups, while the charge density of the PLL segments remained unchanged even after thiolation by Traut's reagent, because the reaction was accompanied by the introduction of cationic imino groups. Consequently, the former system, balancing the densities of charge and disulfide cross-linking, achieved for the first time a remarkable increase in the transfection efficiency compared to non-cross-linked control while maintaining its stability in the extracellular environment.

Experimental Section.

Materials. α-Methoxy-ω-amino-poly(ethylene glycol) (M_w = 12 000) was a kind gift from Nippon Oil and Fats Co., Ltd. (Tokyo, Japan). The PEG-PLL block copolymers with an average polymerization degree of PLL segment of 71 were synthesized as previously described.[4] *N*-Succinimidyl 3-(2-pyridyldithio)propionate (SPDP), dithiothreitol (DTT), and sodium dextran sulfate (M_w = 25 000) were purchased from Wako Pure Chemical Co., Ltd. (Osaka, Japan). 2-Iminothiolane (Traut's reagent) and Micro BCA protein assay reagent kit were purchased from PIERCE Co., Inc. (Rockford, IL). *N*-Methyl-2-pyrrolidone (NMP) was purchased from Aldrich Co., Inc. (Milwaukee, WI). A pGL3 control vector, which was purchased from Promega Co., Inc. (Madison, WI), was used as pDNA in all the experiments. This pDNA was amplified in competent DH5α *Escherichia coli* and purified using HiSpeed Plasmid MaxiKit purchased from QIAGEN Sciences Co., Inc. (Germantown, MD).

Synthesis of Thiolated PEG-PLL. Introduction of thiol groups to the side chain of PEG-PLL was performed using either a heterobifunctional reagent SPDP[13] (Scheme 1a) or a cyclic thioimidate Traut's reagent[14] (Scheme 1b). The typical synthetic procedure is described as follows for the PEG-PLL-PDP (37 mol % substitution): PEG-PLL (51 mg, 1.90 μmol) and SPDP (60 mg, 192 μmol) were separately dissolved in NMP containing 5 wt % LiCl (2 mL for PEG-PLL, 6 mL for SPDP). The solution containing SPDP (2.5 mL) was added to PEG-PLL solution (2 mL) and stirred at room temperature for 24 h after the addition of 10% volume of *N*,*N*-diisopropylethylamine. Then, the mixture was precipitated into an approximately 20-times-excess volume of diethyl ether. The crude precipitate was washed twice with diethyl ether to

(8) Meister, A.; Anderson, M. E. *Annu. Rev. Biochem.* **1983**, *52*, 711−760.
(9) Kakizawa, Y.; Harada, A.; Kataoka, K. *J. Am. Chem. Soc.* **1999**, *121*, 11247−11248.
(10) Kakizawa, Y.; Harada, A.; Kataoka, K. *Biomacromolecules* **2001**, *2*, 491−497.
(11) Trubetskoy, S. V.; Loomis, A.; Slattum, M. P.; Hagstrom, E. J.; Budker, G. V.; Wolff, A. J. *Bioconjugate Chem.* **1999**, *10*, 624−628.
(12) McKenzie, D. L.; Kwok, K. Y.; Rice, K. G. *J. Biol. Chem.* **2000**, *275*, 9970−9977.
(13) Carlsson, J.; Drevin, H.; Axen, R. *Biochem. J.* **1978**, *173*, 723−737.
(14) King, T. P.; Li, Y.; Kochoumian, L. *Prepr. Protein Conjugates* **1978**, *17*, 1499−1506.

obtain white powder. The polymer was dissolved in 0.01 N HCl solution, dialyzed against distilled water overnight, and lyophilized to obtain the final product. The reaction of PEG-PLL with Traut's reagent was carried out in a similar way, e.g., Traut's reagent (20 mg, 145 μmol) in NMP (2 mL) was added to PEG-PLL (29 mg, 1.10 μmol) in NMP (2 mL) to obtain the PEG-PLL-IM (22 mol % substitution). Thiolated PEG-PLLs with different thiolation degrees were obtained by changing molar ratio of SPDP or Traut's reagent to the ϵ-amino groups of PEG-PLL according to the aforementioned method. The degree of the thiol substitution for each thiolated PEG-PLL was determined from the peak intensity ratio of the methylene protons of PEG (OCH_2CH_2, δ = 3.5 ppm) to the pyridyl protons of the 3-(2-pyridyldithio)propionyl groups (C_5H_4N, δ = 7.2−8.3 ppm) or the newly introduced methylene protons of 1-imino-4-mercaptobutyl groups ($HS-(CH_2)_3-C(NH_2^+)^-$, δ = 2.1−3.4 ppm) in ^{1}H NMR spectra taken in D_2O at 25 °C.

Preparation of the Cross-Linked Block Catiomer Polyplex. Each thiolated PEG-PLL was dissolved in 10 mM Tris-HCl buffer (pH 7.4) at 1−2 mg/mL, followed by the addition of 10% volume of 100 mM DTT solution. After a 30 min incubation at room temperature, the polymer solutions were diluted up to the residual molar concentration of the cationic moieties (primary amino and imino groups) to equal 0.615 μmol/mL by the same buffer. Then, the polymer solutions were added to a 2-times-excess volume of 50 μg/mL pDNA solution (0.154 μmol/mL phosphate groups) to form the polyplex at a charge ratio of 2. The final concentration of pDNA in all the samples was adjusted to 33 μg/mL. Charge ratio was defined as the residual molar ratio of positive charge of PEG-PLL or thiolated PEG-PLL to phosphate group of pDNA. After an overnight incubation at room temperature, the polyplex solutions were dialyzed against 10 mM Tris-HCl (pH 7.4) containing 0.5% dimethyl sulfoxide at 37 °C for 24 h to remove the impurities, followed by 2 days of additional dialysis for removal of dimethyl sulfoxide. During the dialysis, the thiol groups of thiolated PEG-PLL were oxidized to form the disulfide cross-links. To follow the process of oxidation, the remaining thiol groups in disulfide cross-linked polyplexes were determined by Ellman's method.[15]

Size of Cross-Linked Block Catiomer Polyplex. To estimate the hydrodynamic diameters of cross-linked block catiomer polyplexes, dynamic light scattering (DLS) measurements were carried out using a DLS-7000 instrument (Otuka Electronics Co, Ltd., Hirakata, Japan). An Ar ion laser (λ = 488 nm) was used as an incident beam. Block catiomer polyplex solutions with a charge ratio of 2 were adjusted to have a concentration of 33 μg pDNA/mL. The data obtained at a detection angle of 90° at 25 °C were analyzed by the cumulant method to obtain the hydrodynamic diameters and polydispersity indices (μ/Γ^2) of the polyplexes.[16]

For AFM imaging of DNA complexes, 4 μL of each sample solution was deposited on a freshly cleaved mica substrate for 30 s. The solution was dried under a gentle flow of nitrogen gas. AFM imaging was performed in tapping mode with standard silicon probes (160 μm in length, Olympus, Tokyo, Japan) on a NVB100 microscope (Olympus) controlled by an operating software of Nanoscope IIIa (Digital Instruments, Santa Barbara, CA). Cantilever oscillation frequency was tuned to the resonance frequency of the cantilever, 260−340 kHz. The 256 × 256 images were recorded at a 0.5−2 μm/s linear scanning speed at a sampling density of 4−60 nm^2 per pixel. Raw AFM images have been processed only for background removal (flattening) using the microscope manufacturer's image-processing software.

Dye Exclusion Assay. Block catiomer polyplex solutions (33 μg pDNA/mL) prepared at a charge ratio of 2 were adjusted to have 10 μg pDNA/mL with 2.5 μg EtBr/mL and 150 mM NaCl by adding 10 mM Tris-HCl (pH 7.4) buffer containing EtBr and NaCl. The solutions were incubated at ambient temperature overnight. Fluorescence measurements of sample solutions were carried out at 25 °C using a spectrofluorometer (FP-6500, Jasco, Tokyo, Japan). Fluorescence intensity of the samples at 590 nm was measured with excitation at 510 nm. Relative fluorescence intensity was calculated as follows:

$$F_r = (F_{sample} - F_0)/(F_{100} - F_0)$$

where F_{sample} was fluorescence intensity for the samples, F_{100} was free pDNA, and F_0 was background.

Gel Retardation Analysis. Sodium dextran sulfate (0.83 mM, M_w = 25 000) in 10 mM Tris-HCl (pH 7.4) buffer was added to the same volume of polyplex solutions (33 μg pDNA/mL) prepared at a charge ratio of 2 in 10 mM Tris-HCl (pH 7.4) buffer to have an approximately 20-times-excess charge ratio of sodium dextran sulfate to pDNA in the mixture. The mixed solution was then diluted up to 8.3 μg pDNA/mL by the same volume of 10 mM Tris-HCl (pH 7.4) buffer with or without 50 mM DTT. After an overnight incubation at 37 °C in a sealed container, 20 μL of each sample (166 ng pDNA) was electrophoresed at 100 V for 1 h on a 0.9 wt % agarose gel in 20 mM Tris-acetic acid buffer containing 10 mM sodium acetic acid (pH 7.8). pDNA in the gel was visualized by EtBr (0.5 μg/mL) staining.

Transfection. 293T cells were plated into six well gelatin-coated culture plates. After a 24 h incubation in 1.5 mL of Dulbecco's modified eagle medium (DMEM) containing 10% serum, the medium was replaced with 1 mL of a transfection medium containing 10% serum and 100 μM hydroxychloroquine. Ninety μL of each polyplex solution (33 μg/mL pDNA) was then applied to each well for the transfection. The amount of pDNA was adjusted to 3 μg per well. After 24 h of incubation, the medium was replaced with 1 mL of the medium containing 10% serum, followed by an additional 24 h incubation. The luciferase gene expression was then evaluated from the intensity of photoluminescence using Fluoroskan Ascent FL system (Labsystems, Helsinki, Finland). The amount of protein in each well was concomitantly determined using a Micro BCA Protein Assay Reagent Kit.

Effect of Freeze−Thawing Process of Polyplexes on Transfection. Polyplex solutions with a charge ratio of 2 were prepared as described in the preceding section to adjust the pDNA concentration of 33 μg/mL. Each sample was frozen at −20 °C for 2 h, followed by thawing at room temperature for 30 min. Both nonfrozen and freeze−thawed polyplexes were subjected to the luciferase transfection assay using 293T cells.

Results and Discussion

Thiolation of PEG-PLL. Thiolated PEG-PLLs were synthesized using two types of thiolation reagents, i.e., SPDP and Traut's reagent. The activated ester of SPDP reacts with the ϵ-amino group of lysine residue, resulting in the introduction of the 3-(2-pyridyldithio)propionyl (PDP) groups via amide linkage into the side chain of the PLL segment of PEG-PLL (Scheme 1a). Consequently, the cationic charge density of the PLL segment was decreased through the thiolation. Samples with varying thiolation degree were prepared by this method and abbreviated as PDP-X, where X stands for the percent thiolation (%) of the ϵ-amino groups calculated from the peak intensity ratio of the methylene protons of PEG (OCH_2CH_2, δ = 3.5 ppm) to the pyridyl protons of the 3-(2-pyridyldithio)-propionyl groups (C_5H_4N, δ = 7.2−8.3 ppm) in ^{1}H NMR spectrum as typically seen in Figure 1 (PDP-37). Treatment of PDP-X with an excess amount of DTT gave the reduced form having flanking 3-mercaptopropionyl groups, which we abbreviated as MP-X.

As an approach of thiolation with keeping the charge density unchanged, the amidination of ϵ-amino groups of PLL segment

(15) Riddles, P. W.; Blakeley, R. L.; Zerner, B. *Anal. Biochem.* **1979**, *94*, 75−81.
(16) Itaka, K.; Yamauchi, K.; Harada, A.; Nakamura, K.; Kawaguchi, H.; Kataoka, K. *Biomaterials* **2003**, *24*, 4495−4506.

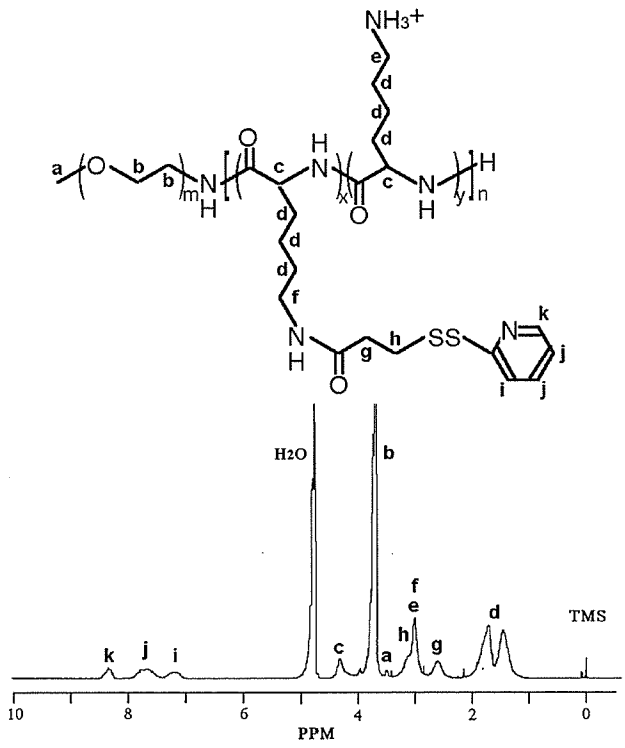

Figure 1. ^{1}H NMR spectrum of PDP-37 (solvent, D_2O; temperature, 25 °C; concentration, 10 mg/mL).

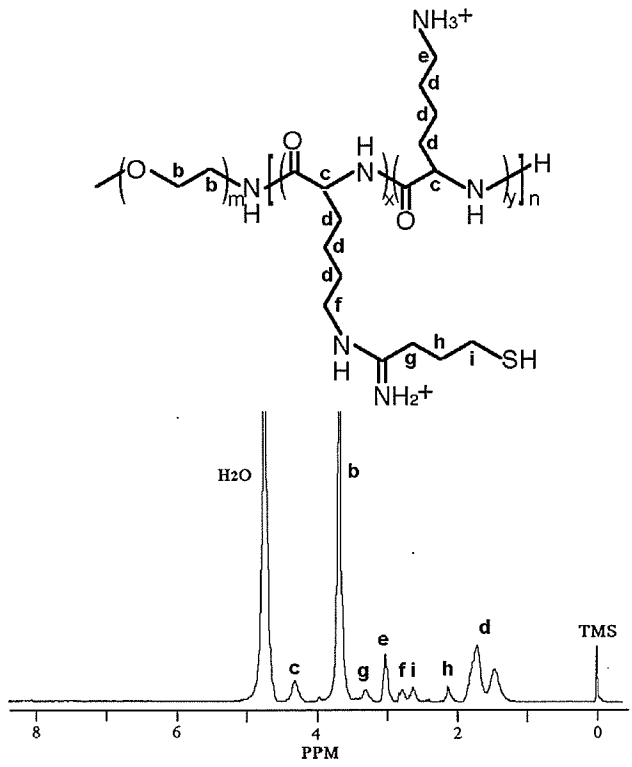

Figure 2. ^{1}H NMR spectrum of IM-22 (solvent, D_2O; temperature, 25 °C; concentration, 10 mg/mL).

was done by Traut's reagent to introduce thiol groups with cationic imino moieties as seen in Scheme 1b. ^{1}H NMR spectrum shown in Figure 2 (IM-22) clearly indicates the introduction of both thiol and imino moieties in the sample from the peaks of newly introduced methylene protons of 1-imino-4-mercaptobutyl groups from Traut's reagent ($HS-(CH_2)_3-C(NH_2^+)^-$, $\delta = 2.1-3.4$ ppm). Thiolated polymers containing 1-imino-4-mercaptobutyl groups were abbreviated as IM-X, where X stands for the percent thiolation.

Table 1. Cumulant Diameters and Polydispersity Indices (μ/Γ^2) of Block Catiomer Polyplexes

	cumulant diameter [nm]	polydispersity index (μ/Γ^2)
PEG-PLL polyplex (non-cross-linked)	102	0.16
IM-X polyplexes (cross-linked)		
IM-9	102	0.15
IM-22	100	0.16
MP-X polyplexes (cross-linked)		
MP-5	103	0.14
MP-13	106	0.14
MP-28	103	0.13
MP-37	115	0.19

Formation of Cross-Linked Block Catiomer Polyplex. The block catiomer polyplexes from pDNA and thiolated PEG-PLL were prepared at the charge ratio of 2, where no free pDNA was observed in an agarose gel retardation analysis (data not shown). To determine the process of oxidative cross-linking, the polyplex samples were subjected to Ellman's test for the estimation of residual thiol groups. After 3 days of dialysis, the amount of remaining thiol groups was calculated to be less than 10% of the initial value for all the samples, indicating that the core of block catiomer polyplexes was cross-linked through covalent disulfide bonds between the side chain of PLL segment of PEG-PLL.

The size and shape of the cross-linked polyplexes were then evaluated by DLS and AFM measurements. Table 1 summarizes the cumulant diameters of the polyplexes determined by DLS, indicating that all of the block catiomer polyplexes, regardless of the cross-linking and charge densities, have diameters around 100 nm with a moderate polydispersity between 0.13 and 0.19. This is in line with the results of the atomic force microscopy (AFM) of the dried polyplexes on a mica disk as seen in Figure 3. A toroidal structure in the size range of 60−100 nm and a rodlike structure with a long axis of 150−300 nm were observed by AFM. Our previous work on polyplex examination by static light scattering revealed that the block catiomer polyplexes of PEG-PLL prepared at a charge ratio of 2 is likely to contain a single pDNA molecule in each of the polyplexes without any secondary coalescence.[16] Present AFM imaging of the polyplexes is reasonably consistent with this previous estimation based on the static light scattering analysis.

Ethidium bromide (EtBr) is known to form an intercalating complex with double helical polynucleotides to show a striking enhancement in its fluorescence intensity.[17] This enhanced fluorescence was quenched upon the condensation of DNA through the complexation with cationic component due to the hindered intercalation of EtBr into double-stranded structure of DNA molecules. Thus, EtBr exclusion assay was frequently utilized to estimate the degree of pDNA condensation in ion complexes.[17,18] As seen in Figure 4, non-cross-linked polyplexes

(17) LePecq, J.-B.; Paoletti, C. *J. Mol. Biol.* **1967**, *27*, 87−106.
(18) Itaka, K.; Harada, A.; Nakamura, K.; Kawaguchi, H.; Kataoka, K. *Biomacromolecules* **2002**, *3*, 841−845.

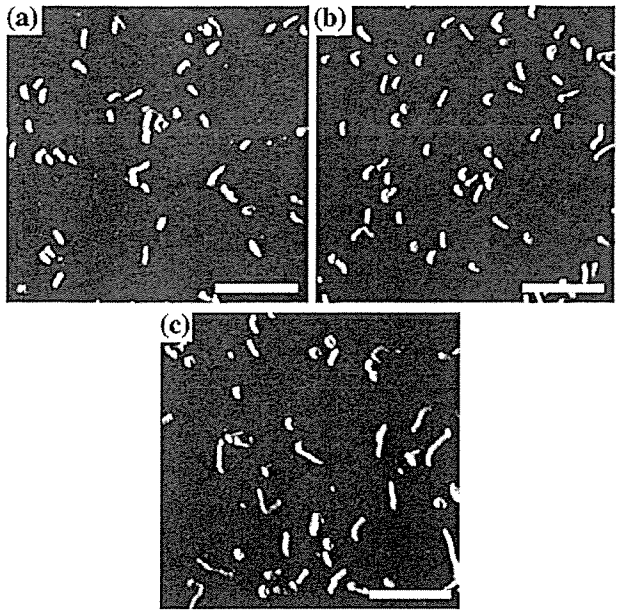

Figure 3. AFM images of block catiomer polyplexes. (a) PEG-PLL polyplex (non-cross-linked), (b) IM-22 polyplex (cross-linked), and (c) MP-28 polyplex (cross-linked). Images are shown in amplitude mode, and all the scale bars are equivalent to 500 nm.

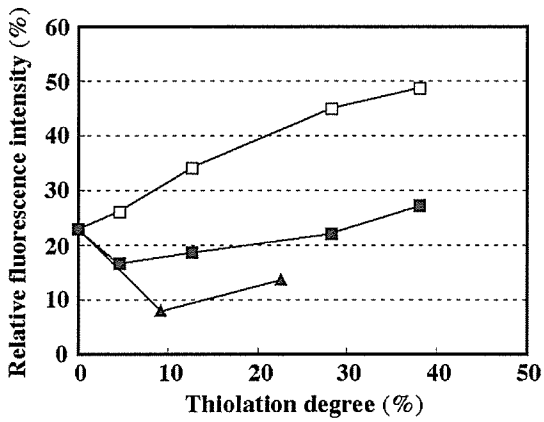

Figure 4. Effect of thiolation degree of non-cross-linked and cross-linked block catiomer polyplexes on the fluorescence intensity of EtBr. Fluorescence measurements were carried out as described in the Experimental Section. (□) PDP-X polyplex, (■) MP-X polyplex, (▲) IM-X polyplex.

from PDP-X showed a monotonic increase in the EtBr fluorescence with an increase in the thiolation degree, indicating a lowered tendency of dye exclusion. This result demonstrates that the decreased charge density of PLL segment through the reaction with SPDP led to a lowered capacity to induce pDNA condensation. On the other hand, the disulfide cross-linked polyplexes from MP-X had a substantially lowered fluorescence intensity than the corresponding non-cross-linked polyplexes from PDP-X and revealed the fluorescence intensity the same as the polyplex from PEG-PLL (nonthiolated polymer), indicating their characteristic to compensate for the decreased cationic charge with disulfide cross-linking. Furthermore, the cross-linked polyplexes from IM-X with a fixed charge density exhibited even lower fluorescence intensity than the cross-linked MP polyplexes with a decreased charge density, showing that the additional disulfide cross-linking to the electrostatic interaction further promotes the condensation of pDNA.

Stability of Cross-Linked Systems. The stability of the cross-linked polyplexes against the counter polyanion exchange reaction may play a key role in pDNA release from the polyplexes in the intracellular compartment and was thus evaluated by the agarose gel electrophoresis as seen in Figure 5. The effects of cross-linking and charge densities on counter polyanion-induced dissociation of the polyplexes in nonreductive and reductive conditions were evaluated by this method. Obviously, in the nonreductive condition (Figure 5a, lane 2 and Figure 5b, lane 2), the bands of the free pDNA (super-coil and open-circular forms) were observed for the non-cross-linked systems (PEG-PLL and PDP-28 polyplexes). On the contrary, the free pDNA bands were not detected in the condition without DTT (Figure 5a, lanes 3 and 4 and Figure 5b, lanes 3−6) for all of the cross-linked systems (IM- and MP-polyplexes), indicating the substantial stabilization of the cross-linked polyplexes against the exchange reaction. Noteworthy is the behavior of MP-28 in the reductive medium containing 25 mM DTT (Figure 5b, lane 9): The free pDNA bands were only clearly observed for this system among all of the cross-linked polyplexes. This result indicates that the release of pDNA through the cleavage of the disulfide cross-linking occurs effectively with the polyplex designed to optimally balance the densities of charge and disulfide cross-linking.

In Vitro Transfection Efficiency of Cross-Linked Block Catiomer Polyplex. To assess the environmental sensitivity in the intracellular compartment, transfection of luciferase gene (pGL3) to cultured 293T cells was then carried out using these cross-linked polyplexes (Figure 6a). The cross-linked polyplexes of IM series, showing no release of entrapped pDNA in the electrophoretic assay under the reductive environment, resulted in an even lower transfection than the non-cross-linked control (PEG-PLL). This indicates that an additional introduction of disulfide cross-links to the polyplex with an appreciably high cationic charge density works synergistically to prevent pDNA release from the polyplex even in the reductive intracellular environment, resulting in a lowered transfection efficiency. Notably, the cross-linked polyplexes of MP series, the system compensating for the decrease in the charge density with the disulfide cross-linking, revealed an increased transfection efficiency compared to PEG-PLL, taking a maximum efficiency at MP-28 to achieve 1 order of magnitude higher luciferase expression than PEG-PLL. Note that this is reasonably consistent with their capability of pDNA release in the reductive environment as demonstrated in electrophoretic assay (Figure 5b). Progressive increase in gene expression with an increased thiolation degree up to 28% for MP series may be ascribed to the facilitated release of pDNA from the polyplex in the intracellular reductive environment due to the decreased charge density of ion-complexed polycation segment. On the other hand, MP-37 apparently revealed a lowered gene expression compared to MP-28. Release of pDNA from MP-37 is likely to be impeded even in the intracellular reductive environment, presumably due to the overstabilization through the excessive disulfide cross-linking. As seen in Figure 6b, PDP-28, the non-cross-linked control of MP-28, revealed only a 2 times higher transfection efficiency than PEG-PLL, indicating that the lowered charge density is not the main reason for the significantly higher efficiency of the MP-28 polyplex. It is reasonable to assume that disulfide cross-links may inhibit the MP-28

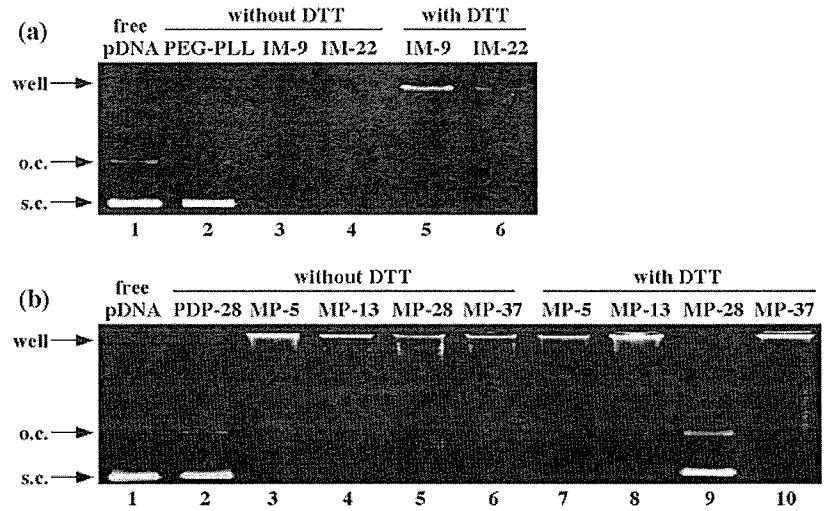

Figure 5. Agarose gel retardation analysis. Each sample was mixed with dextran sulfate (M_w = 25 000, ca. 20 times excess charge ratio to pDNA) and incubated at 37 °C for 24 h, followed by gel electrophoresis (final concentration of pDNA: 8.3 μg/mL). The reductive condition was prepared by adding DTT (25 mM). (a) Retardation assay for IM series. From left: lane 1, free pDNA; lane 2, PEG-PLL polyplex; lanes 3 and 4, IM-X polyplex without DTT; lanes 5 and 6, IM-X polyplexes with 25 mM DTT. (b) Retardation assay for MP series. From left: lane 1, fee pDNA; lane 2, PDP-28; lanes 3–6, MP-X without DTT; lanes 7–10, MP-X with 25 mM DTT. (s.c., supercoiled; o.c., open circular form of pDNA).

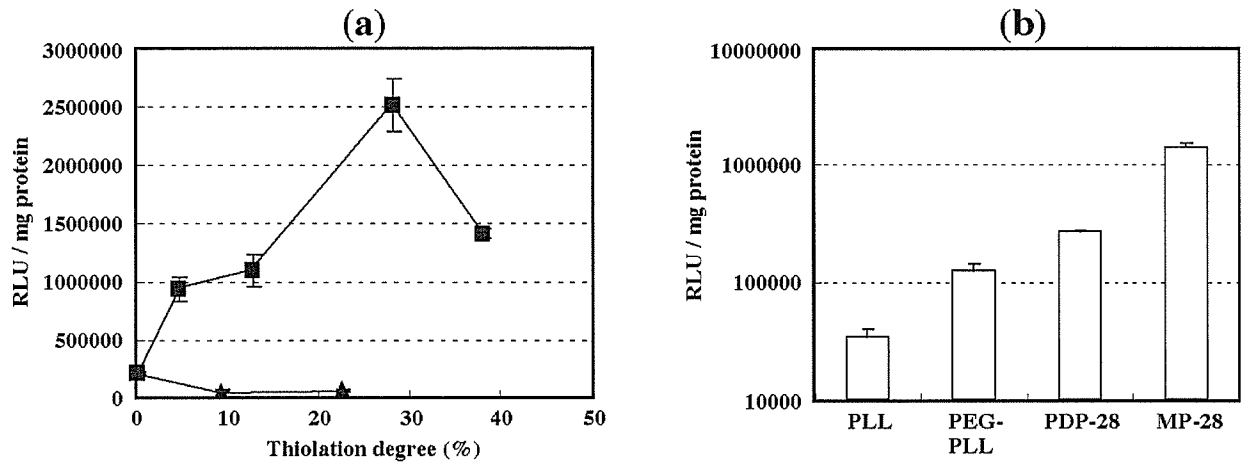

Figure 6. Transfection of luciferase gene to 293T cells by the block catiomer polyplexes. 293T cells were incubated with the polyplexes in the medium containing 100 μM hydroxychloroquine (HC) and 10% serum for 24 h, followed by an additional 24 h culture without the polyplexes and HC in the medium containing 10% serum. (a) Effect of the thiolation degree on the transfection efficiency. (■) MP-X polyplex, (▲) IM-X polyplex. (b) Progressive increase in transfection with a modulation in the structure of PLL-based polyplexes. PLL (poly(L-lysine) homopolymer, M_w = 18 000) was used as the control polyplex.

polyplex from disintegrating in the extracytoplasmic environment, allowing the effective intracellular delivery of pDNA. Subsequently, the cleavage of the disulfide bond in the reductive intracellular compartment triggers the efficient release of pDNA from the MP-28 polyplex, because it should induce a substantial decrease in the association force in the polyplex, a system compensating the decreased charge with disulfide cross-linking.

From a practical viewpoint, long-term storage of gene carriers in a regulatory condition, including powdered and frozen formulations, is a crucial issue. Nevertheless, the conventional lipoplexes and polyplexes are not tolerant of freezing, resulting in a significant loss in the transfection efficiency in the absence of particular saccharide compounds as lyoprotectants.[19–21] As seen in Figure 7, the disulfide cross-linking (MP-28) completely protects the transfection capacity of the block catiomer polyplexes even after the simple freeze–thawing without using any protective reagents. This is in a sharp contrast to the significantly lowered transfection efficiency of non-cross-linked polyplexes after the freeze–thawing process. The disulfide cross-linking obviously prevents the polyplex from the structural change induced by freezing stress. Indeed, there was no substantial change in AFM images of the cross-linked polyplexes before and after the freeze–thawing process (data not shown).

Conclusions

Here, the disulfide cross-linked polyplex is shown to undergo the environment-sensitive release of pDNA through the regulated

(19) Talsma, H.; Cherng, J.-Y.; Lehrmann, H.; Kursa, M.; Ogris, M.; Hennink, W. E.; Cotten, M.; Wagner, E. *Int. J. Pharm.* **1997**, *157*, 233–238.
(20) Cherng, J.-Y.; Wetering, P.; Talsma, H.; Crommelin, D. J. A.; Hennink, W. E. *Pharm. Res.* **1997**, *14*, 1838–1841.
(21) Anchordoquy, T. J.; Carpenter, J. F.; Kroll, D. J. *Arch. Biochem. Biophys.* **1997**, *348*, 199–206.

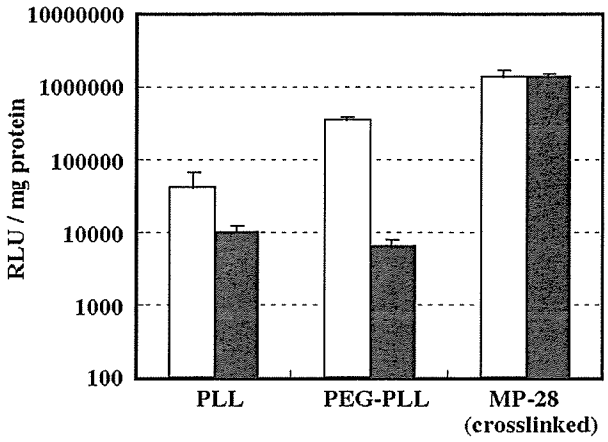

Figure 7. Effect of freeze−thawing on the transfection efficiency of polyplexes. Open bar: nonfrozen sample. Closed bar: freeze−thawed sample. All the polyplex samples were frozen at −20 °C for 2 h, followed by thawing at room temperature for 30 min. PLL represents poly(L-lysine) homopolymer (M_w = 18 000).

cleavage of disulfide bond in the reductive condition. The cross-linked polyplexes with a lowered charge density (MP-X polyplexes), in particular MP-28, achieved significantly higher transfection than those with a fixed charge density (IM-X polyplexes). The presence of the optimal thiolation degree (28%) in MP-X supports our hypothesis that the efficient transfection in the disulfide cross-linked polyplexes can be achieved by controlling the balance between the cationic charge and disulfide cross-linking densities. Our results should provide a comprehensive knowledge of designing the environment-sensitive polyplex systems with high stability in extracellular environments and an effective releasing capacity of pDNA in intracellular compartments for the efficient transfection. Our recent animal study revealed an appreciable gene expression in mouse liver for intravenously injected MP-28, and detailed results will be reported elsewhere in near future.

Acknowledgment. This work was financially supported by the Core Research Program for Evolutional Science and Technology (CREST) from the Japan Science and Technology Corporation (JST) as well as by Special Coordination Funds for Promoting Science and Technology from the Ministry of Education, Culture, Sports, Science and Technology of Japan (MEXT). We express our appreciation to Mr. Hiroshi Nagano, The University of Tokyo, and Mr. Shigeto Fukushima, Nippon Kayaku Co., Ltd., Japan, for their help with the polymer synthesis.

JA0379666

nature
biotechnology

Nanospheres for DNA separation chips

Mari Tabuchi[1,5,6], Masanori Ueda[1,5], Noritada Kaji[1,5], Yuichi Yamasaki[2,5], Yukio Nagasaki[3,5], Kenichi Yoshikawa[4,5], Kazunori Kataoka[2,5] & Yoshinobu Baba[1,5,6,7]

We report here a technology to carry out separations of a wide range of DNA fragments with high speed and high resolution. The approach uses a nanoparticle medium, core-shell type nanospheres, in conjunction with a pressurization technique during microchip electrophoresis. DNA fragments up to 15 kilobase pairs (kbp) were successfully analyzed within 100 s without observing any saturation in migration rates. DNA fragments migrate in the medium while maintaining their characteristic molecular structure. To guarantee effective DNA loading and electrofocusing in the nanosphere solution, we developed a double pressurization technique. Optimal pressure conditions and concentrations of packed nanospheres are critical to achieve improved DNA separations.

Genome projects are accomplished using DNA sequencing systems based on capillary array electrophoresis. However, more powerful and simple analytical systems for separation of biopolymers (DNA fragments and proteins) will be required to rapidly and precisely analyze samples. Although microchip electrophoresis techniques combined with hydrophilic polymer media appear to be promising, particularly for some DNA separations[1,2], the separation of longer DNAs (greater than several kbp) still results in electrophoretic mobility that is independent of length in conventionally available media[3]. Consequently, estimation of DNA size in these systems is ambiguous. In addition, high-viscosity polymer solutions are usually used in these experiments to obtain good resolution, and the handling of these types of solutions can be difficult. Several low-viscosity media[4–10] and various techniques using nanofluidic[11–14] or magnetic[15] structures have been developed to improve biopolymer size separation methodologies.

These methods have led to significant advances in separation technology, such as a poly(dimethylacrylamide) (POP-6^T)[4] for DNA sequencing, and some of them will find practical use in functional genome and proteome projects and clinical applications in the near future. However, these systems are applicable only for separations within a limited size range (less than 1 kbp[4,9] or greater than several kbp[7,8,10–15]) and they require thermo-control[5,6] or other expensive and robust devices[11–15]. Here we describe an effective and simple analytical system based on core-shell type nanosphere technology, which is applicable to separation of DNA fragments across a broad size range.

We recently developed a core-shell type of globular nanoparticle (nanosphere) which was prepared by the multimolecular micellization and subsequent core polymerization of block copolymer of poly(ethylene glycol) with poly(lactic acid) possessing a methacryloyl group at the PLA chain end (PEG_m-β-PLA_n-MA_1; Mw(PEG/PLA) = 6,100/4,000, m ≈ 100, n ≈ 40, l ≈ 70) in aqueous medium[16]. The hydrophobic PLA segments form a spherical core, which is covered by tethered, flexible PEG chains at a fairly high density. The methacryloyl groups located in the particle core were polymerized to form stable core-shell type nanospheres having a diameter of 30 nm (**Fig. 1a**). The nanospheres have no surface charge, and they have a narrow size distribution and low viscosity in aqueous media (0.94 cP at 1.0% (10 mg/ml)) compared with conventional polymers (*e.g.*, methylcellulose: 8.8 cP at 0.5% and 104 cP at 1.0%), owing to their globular structure. We anticipate that these nanoparticles will provide a suitable nano-packing medium for use as a sieving matrix in microchannels. Our calculations show that the nanospheres form a close-packed structure at 1% concentration. Our hypothesis was that densely packed nanospheres with PEG-tethered chains on their surface would improve both the handling properties and the separation of DNA samples, thus providing a method potentially applicable to several high-throughput technologies.

To attain high-speed and improved resolution, we developed a double pressurization technique as an essential component of this nanosphere system. After filling all channels in a microchip with a 1% nanosphere solution, the sample was injected from the vertical direction by initial pressure (P_{1st}) application (P_{1st} = 2.5 kPa for 1 s; **Fig. 1b**, left (i)). Each sample was introduced to the cross section. Just before electrophoretic separation, a secondary pressure (P_{2nd}) was applied for 1 s to the separation channel (P_{2nd} = 2.5 kPa for 1s; **Fig. 1b**, left (ii)), causing the sample at the cross section to advance further as a dispersed broad band without electric field. Subsequently, electrophoresis was done at 220 V/cm (**Fig. 1b**, left (iii) for 0.5 s and (iv) for 1 s) without pressure. The sample band, which initially showed a broad parabolic flow after the P_{2nd} application, was focused by this electrophoretic process to form a plug flow (**Fig. 1b**, left (iii) and (iv)).

[1]Department of Medicinal Chemistry, Faculty of Pharmaceutical Sciences, The University of Tokushima, 1-78 Shomachi, Tokushima 770-8505, Japan. [2]Department of Material Science, Graduate School of Engineering, The University of Tokyo, 7-3-1 Hongo, Bunkyo-ku, Tokyo 113-8656, Japan. [3]Department of Materials Science and Technology, Tokyo University of Science, Noda 278-8510, Japan. [4]Department of Physics, Graduate School of Science, Kyoto University, Kyoto 606-8502, Japan. [5]CREST, Japan Science and Technology Agency, JST, Japan. [6]The 21st Century COE Program, Human Nutritional Science on Stress Control, The University of Tokushima, Tokushima, Japan. [7]Single-molecule Bioanalysis Laboratory, National Institute of Advanced Industrial Science and Technology, AIST, Hayashi-cho 2217-14, Takamatsu, 761-0395, Japan. Correspondence should be addressed to M.T. (tabuchi@ph.tokushima-u.ac.jp).

Published online 8 February 2003; doi:10.1038/nbt939

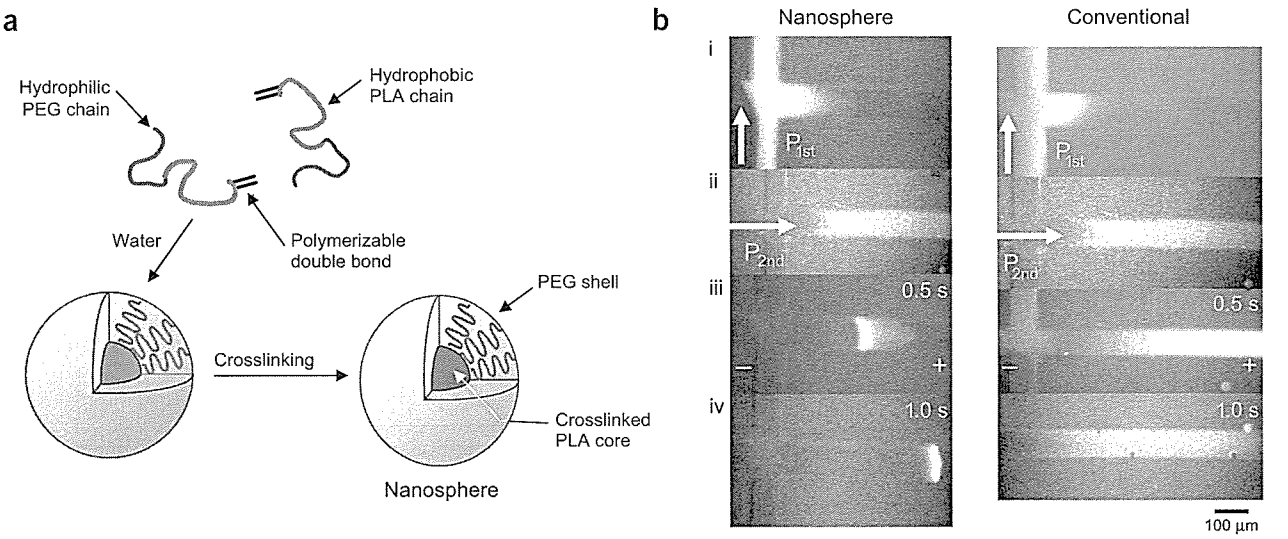

Figure 1 The new system using nanospheres and a double pressurization technique. (**a**) Images of the core-shell type nanosphere structure (nanosphere). (**b**) Fluorescence images taken during application of the double pressurization technique. We observed the sample plug formation (20 ng/μL of 200 bp DNA from Genesura Laboratories with 0.8 μM of the fluorescent dye YOYO1 (Molecular Probes) in 4% 2-mercaptoethanol in TE buffer). Arrows show the pressure application. The horizontal channel is a separation channel. (i) P_{1st}: 2.5 kPa, 1s; after filling all channels with solution (1% nanosphere solution (left), 0.5% methylcellulose (right)) the sample was injected by P_{1st} for 1 s using a syringe from the bottom well of the loading channel, with the top and right wells open. (ii) P_{2nd}: 2.5 kPa, 1s; the sample band introduced into the cross section was advanced by P_{2nd} for 1 s from the left well and in the right direction with the top and bottom wells open. (This places the sample between the layers of the nanospheres (left).) (iii) Electrophoretic separation: 160 V/cm, 0.5 s. (iv) Electrophoretic separation: 160 V/cm, 1 s.

The usual electrokinetic injection of samples without pressurization onto the nanosphere solutions could not generate a sufficiently intense band and no peaks appeared (data not shown). When the same pressurization technique was applied to the conventional polymer solution, the focusing of the broad band did not occur (**Fig. 1b**, right). The electrofocusing, which was observed only in the nanosphere system, seems to be a stacking effect of the packed nanospheres.

Figure 2a shows an electropherogram of DNA fragments generated using both conventional media and nanospheres. High-speed separation of DNA fragments was attained using nanospheres (60 s in nanosphere medium versus 130 s in conventional polymer medium for 100–1,000 bp (**Fig. 2a**, left) and 100 s in nanosphere medium versus 200 s in conventional polymer medium for a 1–15 kbp DNA ladder (**Fig. 2a**, right)). The DNA strands whose mobility is independent of length in conventional polymer solutions (800–1,000 bp for a 100–1,000 bp DNA ladder (**Fig. 2a**, left) and 6–15 kbp for a 1–15 kbp DNA ladder (**Fig. 2a**, right)) were successfully eliminated by the nanospheres. A wide range of DNA fragments between 1 and 15 kbp was successfully analyzed within 100 s without observing any saturation in migration rates.

All peaks over a wide range of DNA fragment sizes (1–15 kbp) were separated by adjusting the initial pressure conditions (P_{1st}: 10 kPa for 1 s, **Fig. 2a** (top right)). As the P_{2nd} was increased from 1 kPa to 10 kPa, the migration time decreased while resolution was retained (for 100 bp double-stranded DNA (dsDNA) ladder: 1 kPa within 150 s; 5 kPa, 90 s; and 10 kPa, 60 s; and for 1 kbp dsDNA ladder: 1 kPa within 180 s; 5 kPa, 140 s; and 10 kPa, 100 s). This suggests that the migration time is dependent upon the degree of pressurization, which may result in a shortened overall effective channel length. However, when a commercially available polymer solution was used, application of P_{2nd} above 2.5 kPa produced broad peaks and the resolution was reduced.

The log-log plots of the relative mobility versus DNA fragment size[17] show that the 'nanospheres with pressurization' method is clearly different from conventional methods (**Fig. 2b**). A prolonged inverse proportional relationship was observed (**Fig. 2b**, [▲]), whereas routine methods using a conventional polymer resulted in a plateau of size-based mobility (**Fig. 2b**, [○]). There was no plateau region (that is, region of 'length-independent electrophoretic mobility') in the range of DNA sizes measured in this study for nanospheres with pressurization. Although some techniques using ultra-diluted polymer solutions and end-labeled free solution electrophoresis methods have produced improvements in migration decay (loss of resolution)[7,9], it is impossible to accurately analyze a broad range of DNA fragment sizes using these methods. The nanosphere and pressurization technique now makes it possible to analyze a broader range of DNA fragment sizes without compromising either the time required for analysis or the migration saturation.

To further analyze the differences in DNA migration in nanosphere solutions versus conventional gels, we visualized the migration of a single DNA molecule directly by fluorescence microscopy (**Fig. 3**). Surprisingly, under an electric field the segregated DNA molecules maintained a 'relaxed' conformation with minimal stretching motion in the nanosphere solution (**Fig. 3a**), in contrast to the usual behavior of DNA in a conventional gel, which involves repetitive stretching and contraction (**Fig. 3b**). Usually, long fragments of DNA in conventional matrices (gels or polymers) align in the direction of the electric field and migrate headfirst, showing an I- or U-shaped DNA structure, which will always involve some stretching[18–20].

The characteristic behavior of DNA in nanospheres indicates that the mechanism of long DNA separation is fundamentally different from traditional mechanisms (**Fig. 3a**). The DNA molecules exhibit intrachain segregation[21], where folded compact regions (mini-globules) and unfolded coil regions coexist within a single DNA (**Fig. 3a**,

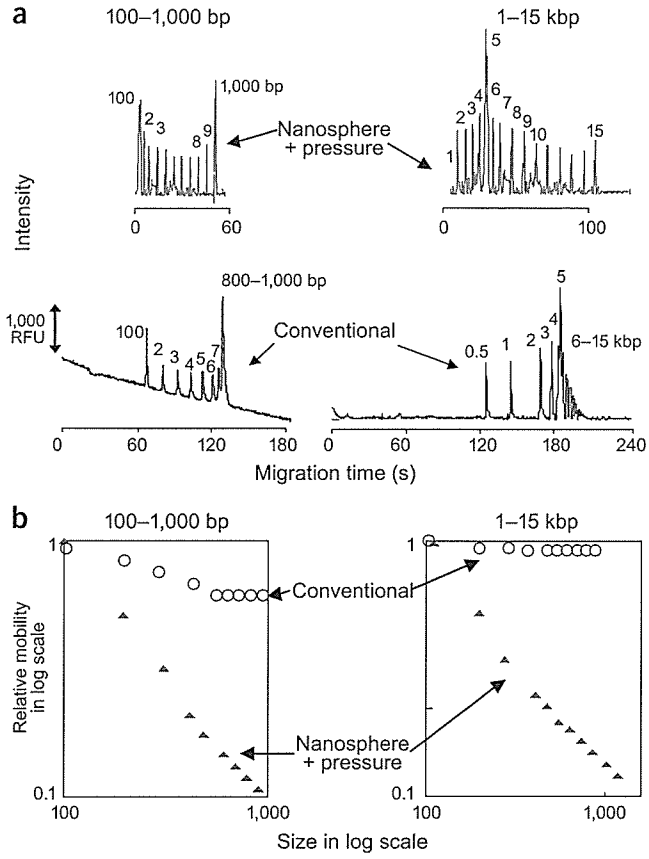

Figure 2 Effectiveness of DNA separations carried out using conventional polymers versus nanospheres with pressurization methods. (**a**) Electropherograms are shown for the following samples. A 1 μg/ml solution of a 100 bp dsDNA ladder containing 10 fragments (Nonagen; 100–1,000 bp; the 100 and 1,000 bp bands are strong) in a 1% (10 mg/ml) nanosphere solution, pH 9, P_{1st}: 2.5 kPa and P_{2nd}: 2.5 kPa (upper left). A 1 μg/mL solution of a 1 kbp dsDNA ladder containing 15 fragments (Nonagen; 1–15 kbp; the 5 kbp band is strong) in a 1% (10 mg/mL) nanosphere solution, pH 9, P_{1st}: 10 kPa and P_{2nd}: 10 kPa (upper right). The 100 bp dsDNA ladder in a conventional polymer (0.5% methylcellulose) solution using conventional electrophoresis (lower left). The 1 kbp dsDNA ladder in a conventional polymer (0.5% methylcellulose) solution using conventional electrophoresis (lower right). (**b**) Log-log plots of the relative mobility versus DNA fragment size. The 100–1,000 bp dsDNA ladder (left), the 1–15 kbp dsDNA ladder (right) for the conventional polymer using conventional electrophoresis [O] and the nanosphere solution with double pressurization method [▲]. RFU, relative fluorescent units.

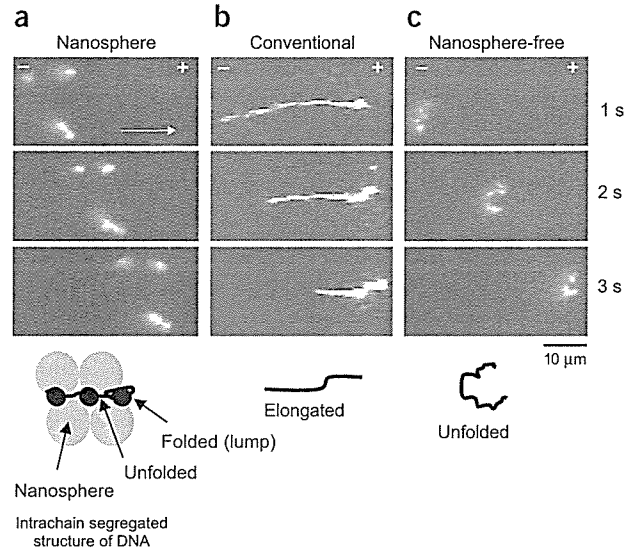

Figure 3 Visualization of single DNA molecules. (**a**,**b**) Sequential fluorescent images of DNA migration behavior (T4 DNA, 165.6 kbp, Takara Bio) under an electric field (10 V) in a 1% nanosphere solution (**a**), a conventional agarose gel (**b**) (1% agarose NA (Amersham Pharmacia Biotech AB), and a control buffer containing no nanospheres (**c**). An illustration of typical DNA conformation is given at the bottom of each figure.

bottom). Note that this intrachain segregated structure also appears in the nanosphere solutions without an electric field, but does not appear in a nanosphere-free solution with (Fig. 3c) or without the electric field, indicating that the nanosphere matrix itself provides the environment required to induce this phenomenon. Because the close-packed structure of nanospheres includes dense regions and a limited amount of extra space, the unfolded coil structure was seen along with regular lumps of DNA (Fig. 3a, bottom). The stretching of DNA is minimal in the nanosphere solution, a consequence of the confined environment, even under an electric field. As a result, DNA molecules migrate while maintaining an intrachain segregated structure within the nanospace. However, to attain such separations, it was necessary to work out optimized conditions for the nanosphere solution. For example, a dilute solution of nanospheres (<1%), in which wider spaces exist between nanospheres, did not produce adequate separations. An effective nanospace is produced by optimizing the concentration of packed nanospheres, which is critical to achieve improved DNA separations. Under optimal packing conditions, physical interaction between the lumps of DNA and the nanospheres might occur, an interaction that may be responsible for the size separation observed. However, a theoretical explanation for the separation method described here has not yet been obtained.

Besides the characteristic intrachain segregated structure seen in nanospheres, the pressurization technique also seems to have contributed to the improved DNA separation, given that both a nanosphere medium and precisely controlled pressurization were needed for the system to work (Fig. 1b). A double pressurization technique was specially developed for microchip electrophoresis using nanospheres. When the P_{1st} and/or P_{2nd} pressurization were not applied, the separation was impossible or was inadequate. The pressurization technique with the nanospheres is the methodology that leads to effective DNA loading, electrofocusing and a shortened effective channel length (Fig. 1b). In addition, adjustment of the pressure force enabled the separation of a wide range of DNA fragments without saturation of migration rates (Fig. 2a). This seems to indicate that nanospaces between nanospheres can be optimized by the pressurization technique. Therefore, the pressurization technique is an essential component of this nanosphere system methodology.

In conclusion, the nanosphere system described here readily separates DNA fragments over a wide range of sizes with higher speed than conventional methods. To use the nanospheres for microchip electrophoresis, samples have to be introduced initially under pressure. Before electrophoretic separation, a secondary application of pressure to the nanospheres accelerates the separation speed of the DNA. The introduced DNA fragments migrate and became focused within the nanosphere solutions under an electric field. The characteristic

'lumps' of DNA intrachain segregated structures are generated in a specific environment of condensed nanospheres. This technology should find wide use in high-throughput analytical systems, including medical diagnoses involving biopolymer analysis. The low viscosity, effective, core-shell type nanosphere method is fully competitive with, and in many cases superior to, conventional separation techniques currently used for analysis of DNA and other biopolymers.

METHODS

Microchip electrophoresis conditions. A microchip electrophoresis system (SV1100 Hitachi Electronics Engineering) and a microchip (i-chip 3; Hitachi Chemical), made of poly(methyl methacrylate) with channels 100 μm wide and 30 μm deep, and a 30 mm effective separation channel were used. In conventional separations, after samples were loaded by voltage (300 V), a separation voltage (890 V) was applied to the separation channel and a squeezing voltage (130 V) was applied to the cross section. The electrophoresis was done at 25 °C. For the new method, after filling all channels on a microchip with a 1% nanosphere solution, the sample was placed at the sample well and was injected into the channels by a P_{1st} application (1–10 kPa for 1s) using a syringe, with the opposite and outlet wells open. Just before electrophoretic separation, P_{2nd} (1–10 kPa for 1 s) was applied to the separation channel from the inlet without an electric field. Subsequently, electrophoresis was done at 220 V/cm with a squeezing voltage of 130 V without pressure (**Supplementary Methods** and **Supplementary Fig. 1** online).

Direct observation of a migrating single DNA. An inverted fluorescence microscope (Axiovert 135TV, Carl Zeiss) was used for direct observation of a single migrating DNA molecule, and fluorescence images were taken to illustrate the results of the various injection modes. Electric fields generated by a multifunction synthesizer (1942, NF Corp.) were applied between the two platinum electrodes through a high-speed power amplifier bipolar power supply (4020, NF CORPORATION). A HVS448 High Voltage Sequencer, LabSmith (HVS448 High Voltage Sequencer) was used to analyze the injection modes.

Note: Supplementary information is available on the Nature Biotechnology website.

ACKNOWLEDGMENTS

This work was partially supported by a grant funding Core Research for Evolutionary Science and Technology from the Japan Science and Technology Agency, a grant from the New Energy and Industrial Technology Development Organization of the Ministry of Economy, Trade and Industry, Japan, a Grant-in-Aid for Scientific Research from the Ministry of Education, Science and Technology, Japan, and the 21st Century COE Program, Human Nutritional Science on Stress Control, Tokushima, Japan. We thank Chie Kuwahara, Ryosuka Kodaka and Fumiko Aboshi of the Tokyo University of Science and Eduardo Jule of the University of Tokyo for preparing the nanospheres. The authors would like to thank Tomoaki Hino, Ken Hirano, Fung Xu, Mohammad Jabasini, Hideya Nagata, Yasuko Tanaka and Emi Endo of the University of Tokushima for technical and secretarial assistance.

COMPETING INTERESTS STATEMENT

The authors declare that they have no competing financial interests.

Received 21 October; accepted 24 November 2003
Published online at http://www.nature.com/naturebiotechnology/

1. Wehr, T., Zhu, M. & Mao, D.T. in *Capillary Electrophoresis of Nucleic Acid*, vol. I (eds. Mitchelson, K.R. & Cheng, J.) 167–187 (Humana Press, Totowa, NJ, 2001).
2. Viovy, J.L. & Dukc, T. DNA electrophoresis in polymer solutions: ogston sieving, reptation and constraint release. *Electrophoresis* **14**, 322–329 (1993).
3. Slater, G.W., Desruisseaux, C. & Hubert, S.J. in *Capillary Electrophoresis of Nucleic Acid*, vol. I (eds. Mitchelson, K.R. & Cheng, J.) 27–34 (Humana Press, Totowa, NJ, 2001).
4. Madabhushi, R.S. Separation of 4-color DNA sequencing extension products in noncovalently coated capillaries using low viscosity polymer solutions. *Electrophoresis* **19**, 224–230 (1998).
5. Lie, Y. & Rill, R.L. in *Capillary Electrophoresis of Nucleic Acid*, vol. I (eds. Mitchelson, K.R. & Cheng, J.) 203–213 (Humana Press, Totowa, NJ, 2001).
6. Buchholz, B.A. *et al.* Microchannel DNA sequencing matrics with a thermally controlled "Viscosity switch." *Anal. Chem.* **73**, 157–164 (2001).
7. Barron, A.E., Blanch, H.W. & Soane, D.S. A transient entanglement coupling mechanism for DNA separation by capillary electrophoresis in ultradilute polymer solution. *Electrophoresis* **15**, 597–615 (1994).
8. Hubert, S.J., Slater, G.W. & Viovy, J.-L. Theory of capillary electrophoretic separation of DNA using ultradilute polymer solution. *Macromolecules* **29**, 1006–1009 (1996).
9. Heller, C. *et al.* Free-solution electrophoresis of DNA. *J. Chromatography A* **806**, 113–121 (1998).
10. Ren, H. *et al.* Separation DNA sequencing fragments without a sieving matrix. *Electrophoresis* **20**, 2501–2509 (1999).
11. Volkmuth, W.D. & Austin, R.H. DNA electrophoresis in microlithography arrays. *Nature* **358**, 600–602 (1992).
12. Chou, C.-F. *et al.* Sorting by diffusion: an asymmetric obstacle course for continuous molecular separation. *Proc. Natl. Acad. Sci. USA* **23**, 13762–13765 (1999).
13. Han, J. & Craighead, H.G. Separation of long DNA molecules in a microfabricated entropic trap array. *Science* **288**, 1026–1029 (2000).
14. Hung, L.R. *et al.* A DNA prism for high-speed continuous fractionation of large DNA molecules. *Nat. Biotechnol.* **20**, 1048–1051 (2002).
15. Doyle, P.S., Bibette, J., Bancaud, A. & Viovy, J.-L. Self-assembled magnetic matrices for DNA separation chips. *Science* **295**, 2237 (2002).
16. Iijima, M., Nagasaki, Y., Okada, T., Kato, M. & Kataoka, K. Core-polymerized reactive micelles from heterotelechelic amphiphilic block copolymers. *Macromolecules* **32**, 1140–1146 (1999).
17. de Gennes, P.G. Reptation of a polymer chain in the presence of fixed obstacles. *J. Chem. Phys.* **55**, 572–579 (1971).
18. Schwartz, D.C. & Koval, M. Conformational dynamics of individual DNA molecules during gel electrophoresis. *Nature* **338**, 520–522 (1989).
19. Smith, S.B., Aldridge, P.K. & Callis, J.B. Observation of individual DNA molecules undergoing gel electrophoresis. *Science* **243**, 203–206 (1989).
20. Shi, X., Richard, R.W. & Morris, M.D. DNA conformational dynamics in polymer solutions above and below the entanglement limit. *Anal. Chem.* **67**, 1132–1138 (1995).
21. Yoshikawa, K. Controlling the higher-order structure of giant DNA molecules. *Adv. Drug Del. Rev.* **52**, 235–244 (2001).